Report SDSMT/IAS/R-93/04 December 1993

RESEARCH RELATED TO THE NORTH DAKOTA THUNDERSTORM PROJECT AND THE NORTH DAKOTA TRACER EXPERIMENT

By: Paul L. Smith, Andrew G. Detwiler,
Mark R. Hjelmfelt, Fred J. Kopp,
L. Ronald Johnson, Harold D. Orville,
and Daran L. Rife

Prepared for:

North Dakota Atmospheric Resource Board
900 East Boulevard Avenue
Bismarck, ND 58505-0850

Contract No. ARB-IAS-92-1

Institute of Atmospheric Sciences

South Dakota School of Mines and Technology

501 East St. Joseph Street

Rapid City, South Dakota 57701-3995

ABSTRACT

Research conducted as part of the North Dakota component of the Federal/State Cooperative Program in Atmospheric Modification Research, funded through NOAA, is summarized. The basic objective of the program is to develop improved techniques for evaluating operational weather modification projects. The North Dakota work concentrates on convective-cloud seeding projects and uses data collected in association with the North Dakota Cloud Modification Project. Continuing analysis of data from the 1989 North Dakota Thunderstorm Project (NDTP) and planning for the 1993 North Dakota Tracer Experiment were the most important activities during the period of this contract. This report summarizes progress in the analysis of data from the NDTP aircraft studies and weather radar data, as well as in numerical cloud modeling and other related studies. Some analyses of data from earlier field projects also continued.

TABLE OF CONTENTS

TABLE OF CONTENTS (continued)

LIST OF FIGURES

1. INTRODUCTION

This report summarizes progress in continuing research efforts aimed at developing improved evaluation techniques for operational weather modification programs. This research is part of the Federal/State Cooperative Program in Atmospheric Modification Research (Reinking, 1985, 1992; Reinking and Meitin, 1989) and is funded by NOAA through a cooperative agreement with the North Dakota Atmospheric Resource Board. The research is closely coordinated with the operational North Dakota Cloud Modification Project (NDCMP), which is also managed by the Board. Major participants in the North Dakota program, in addition to the Board, have included North American Weather Consultants, the South Dakota School of Mines and Technology (SDSM&T), the University of North Dakota (UND), and Weather Modification, Inc., as well as some NOAA scientists. Activities over the past few years have focused on the North Dakota Thunderstorm Project (NDTP; Boe *et al.*, 1992); the field phase was conducted in the area around Bismarck during the summer of 1989, and data analysis efforts have continued since that time. Research carried out by the SDSM&T under the North Dakota program prior to the NDTP is summarized in papers by Miller *et al.* (1983) and Smith *et al.* (1985b, 1989), and a series of reports ending with Smith *et al.* (1990). Earlier SDSM&T research studies associated with the NDTP are summarized in Smith *et al.* (1991a, 1992a,b,c).

Recent scientific emphasis in the North Dakota program has been placed on gaining a better understanding of the transport, dispersion, entrainment, and mixing processes taking place inside convective clouds. This knowledge is needed to understand how glaciogenic seeding agents, dispensed primarily at cloud base in the NDCMP, are delivered to the active supercooled parts of the clouds where they can accelerate the development of precipitation-sized particles through ice processes. The transport processes are also of interest in connection with questions about the mechanisms of hailstone embryo development in feeder clouds and the subsequent transfer of the embryos into the primary hail growth regions.

The recent North Dakota investigations have emphasized field experiments using a sulfur hexafluoride (SF_6) tracer gas dispensed into the clouds and airborne SF_6 analyzers to follow the transport and dispersion processes inside them. Simultaneous release of silver iodide (AgI) seeding aerosols provides "tagged" regions containing artificial ice nuclei and thereby permits concurrent investigation of the nuclei activation processes in the clouds. Radar chaff, fluorescent beads, and natural trace gases were included as additional tracers in the NDTP studies, and the results of releases from ground locations were also investigated with the tracer methods. The NDTP also included some basic studies of convective-storm

dynamic, microphysical, and electrification processes using aircraft, radar, and other observing systems.

The present contract covered the period 1 May 1992 - 31 Dec 1993. The main efforts during this period involved analysis of data from the North Dakota Thunderstorm Project field campaign and planning for the North Dakota Tracer Experiment (NDTE) conducted in the summer of 1993. The analysis of weather radar data from an earlier project carried out in the Dickinson, North Dakota, area in the summer of 1987 also continued. Numerical cloud modeling studies were continued to aid in explaining the basic transport and dispersion processes. These studies complement the field experiments by attempting to simulate the tracer experiments in order to gain increased understanding of the transport and dispersion processes throughout the full volume of the clouds.

The next section of this report presents brief summaries of these activities. Copies of some relevant publications, along with abstracts of other documents completed during the period, are included as appendices.

2. RESEARCH ACTIVITIES

The research effort for the contract period was organized around a set of specified milestones. Section 2.1 reviews the progress toward accomplishment of those milestones. Sections 2.2 and 2.3 provide some further background on the NDTP and the transport and dispersion studies. Section 2.4 reviews progress in some radar data analysis tasks not fully reflected in the list of milestones, while Sections 2.5 through 2.8 list some other activities during the contract period.

2.1 Summary of Contract Milestones

The milestones established as part of this contract are listed below, together with a statement of the progress made towards the completion of each.

Task No.	Target Date	Task Description [Summary of Progress]
ND 92-4	01 June 92	Submit conference paper on 6 July 1989 NDTP case to International Conference on Clouds and Precipitation. [A paper entitled "Observations of Microphysical Evolution in a High Plains Thunderstorm" was submitted for inclusion in the Conference preprint volume. A copy of the paper appears in Appendix A.]

ND 92-5	01 June 92	Submit conference paper on 27 June 1989 NDTP case to International Conference on Nucleation and Atmospheric Aerosols. [A paper entitled "Ice-producing Processes in North Dakota Clouds" was submitted for inclusion in the Conference preprint volume; Appendix B presents a copy of the paper.]
ND 92-9	15 Aug 92	Submit requests to NSF for field facilities in support of NDTE. [Requests were submitted to the NCAR Atmospheric Technology Division for a C-band radar and a mobile CLASS sounding facility, and to South Dakota School of Mines and Technology for T-28 aircraft support, for the NDTE.]
ND 92-10	30 Aug 92	Present papers at International Conferences. [The papers indicated under Tasks 92-4 and 92-5 above were presented at the respective International Conferences during August. Revised versions of both papers were subsequently submitted and accepted for publication in forthcoming special issues of Atmospheric Research; abstracts of the respective manuscripts appear in Appendices C and D.]
ND 92-12	31 Oct 92	Submit journal manuscript on 17 July 1989 NDTP case. [An M.S. thesis and a previous conference paper summarized the analysis of the Doppler radar data for the 17 July NDTP case. However, recently-discovered errors in some of the Doppler analysis software and boundary-related problems in a 3-D model simulation of the case have delayed the preparation of any summary manuscript.]
ND 92-15	15 Nov 92	NDTE planning meeting conducted. [An NDTE planning meeting was held in Rapid City on 28-29 October 1992. Plans for facilities and field operations were discussed and updated.]

ND 92-17	31 Jan 93	Complete draft journal manuscript on 28 June 1989 NDTP lightning study. [A previous M.S. thesis summarizes the lightning data; the journal manuscript has not been completed.]
ND 92-18	31 Mar 93	Prepare conference paper on 10 July 1989 NDTP case. [A paper entitled "Radar and Aircraft Investigation of a North Dakota Thunderstorm Project Complex (10 July 1989)" was submitted for presentation at the 26th International Conference on Radar Meteorology. A copy of the paper appears in Appendix E.]
ND 92-19	31 Mar 93	Finalize field plans for NDTE. [Four SDSM&T participants attended an NDTE planning meeting in Bismarck on 24-25 February, to help complete plans for the field project.]

2.2 North Dakota Thunderstorm Project

The North Dakota Thunderstorm Project (NDTP) field phase was conducted in the central Dakotas during the summer of 1989; Boe *et al.* (1992) provide an overview of the project. The Operations Center was located at the Bismarck, ND, airport. Project aircraft and most personnel were based in Bismarck, with Doppler radars located at Bismarck, Center, and New Salem. The field project began on 12 June and continued through 22 July 1989. A substantial fraction of the SDSM&T Institute of Atmospheric Sciences (IAS) staff participated in the NDTP field effort, as did significant contingents from the Universities of Maryland, North Dakota, and Wyoming, the National Center for Atmospheric Research (NCAR), the NOAA Wave Propagation Laboratory, North American Weather Consultants, and the Atmospheric Resource Board. An NSF Research Experiences for Undergraduates (REU) grant also brought 10 university students to the project (Orville and Knight, 1992).

The NDTP field effort was generally regarded as quite successful. Many of the planned experiments were executed numerous times, although a shortage of mature thunderstorm systems with well-defined feeder clouds limited the opportunities for some of the planned tracer experiments. This probably is a reflection of the fact that central North Dakota remained in the grip of drought during the summer of 1989. The most widespread severe convection occurred on 28 June 1989, and data from that day have been investigated by many NDTP participants. Boe and Johnson (1990) and Frisch *et al.* (1992) studied some of the environmental conditions leading

up to the convective outbreak. Klimowski and Marwitz (1990, 1992a) and Klimowski (1993) conducted Doppler radar studies of a squall line that occurred on 28 June. Nair (1991) and Farley *et al.* (1993) conducted extensive numerical modeling and observational studies of the 28 June storm. Klimowski and Marwitz (1992b) examined the kinematics of a gust front on this day, while Orville *et al.* (1990) studied the development of ice in one of the cells and Helsdon (1990) investigated the overall lightning activity of the day. Moreover, the day was chosen as one of the case study days for investigation by participants in the Third International Cloud Modeling Workshop, held in Toronto in August 1992.

Another NDTP analysis effort examined the formation of a squall line from a broken area of convective storms. Analysis of a storm system that developed over the NDTP network on 17 July 1989 (Chou, 1991; Hjelmfelt *et al.*, 1992) revealed the importance of an atmospheric convergent boundary in organizing the storms into a squall line. Figure 1 shows a sequence of low-level PPI displays from the CP-4 radar near Center on 17 July. At 1313 CDT the radar shows a broken area of convective storms about 50-100 km west of the radar. Farther to the west, an arc of low-reflectivity echo reveals the presence of an atmospheric convergence boundary associated with a synoptic-scale surface trough lying roughly north-south through Dickinson (150 km west of the radar) on the 18 UTC (13 CDT) surface map. The subsequent series of PPI displays, taken at 1358, 1409, and 1423, respectively, shows that this broken area of convection becomes organized into a well-defined narrow, vigorous squall line as the convergence boundary overtakes the storms.

Analysis revealed that the role of the atmospheric convergence boundary in organizing the broken area of storms into a squall line was consistent with the vorticity-balance theory of Rotunno *et al.* (1988). Given that the important role ascribed to the atmospheric convergence boundary in this case is consistent with theory, and that an apparently similar role in squall-line development was played by a (gust front) boundary on 28 June 1989, it appears that this role may be broadly applicable. This is especially so since development from broken areas of convective storms represents a primary formation mechanism for squall lines (Bluestein and Jain, 1985).

Hirsch (1989) compiled a data inventory for the entire NDTP. An overview was included in a paper by Smith *et al.* (1991b) which appeared in the preprint volume of the Second Yugoslav Conference on Weather Modification, and a more comprehensive summary of the project was published in Boe *et al.* (1992). Results from the NDTP provided much of the basis for planning the experiments for the NDTE.

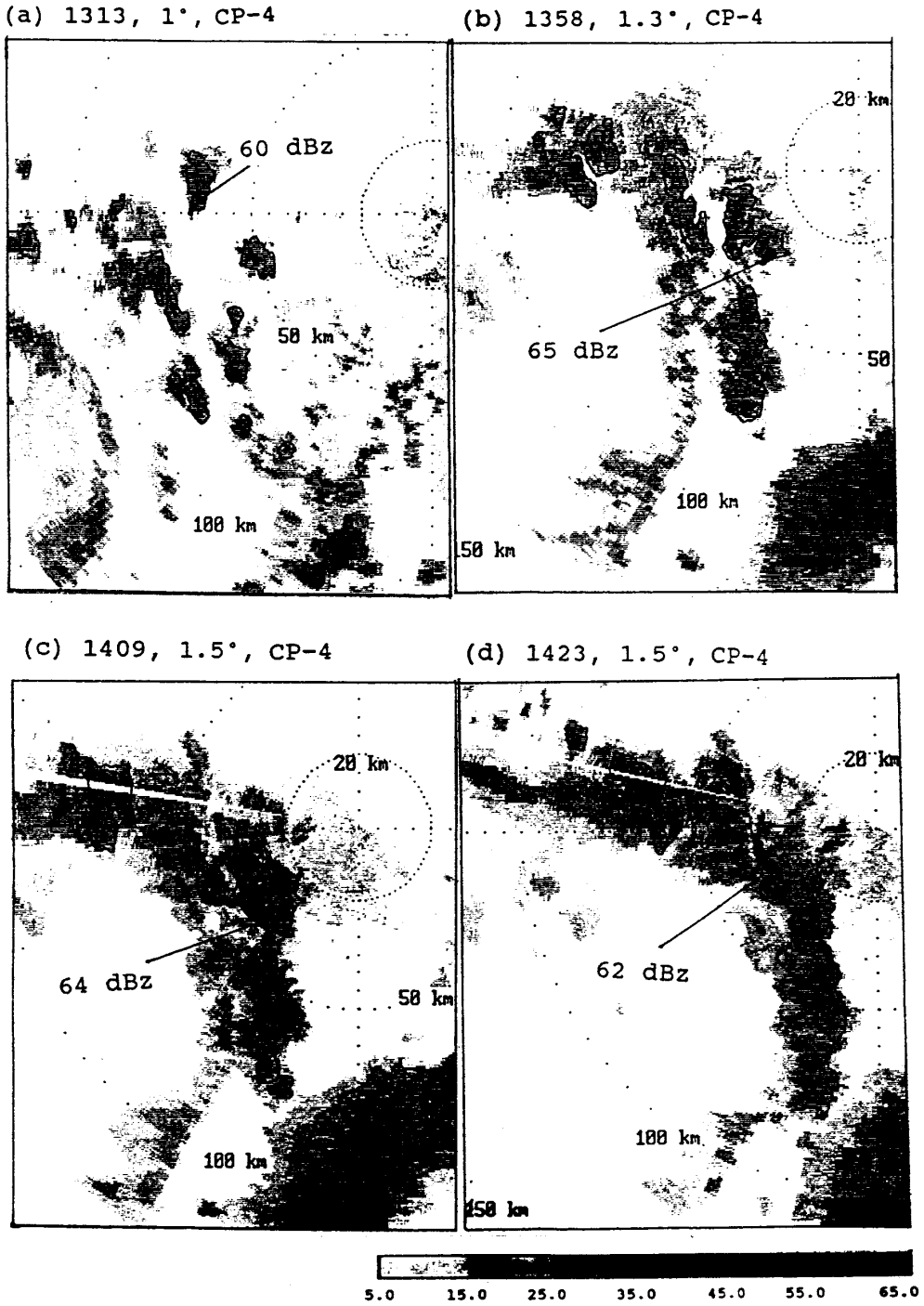

Fig. 1: Low-level radar reflectivity PPI displays at (a) 1313; (b) 1358; (c) 1409; (d) 1423 CDT on 17 July 1989. Reflectivity scale is indicated at the bottom; the 35 and 55 dBz contours are highlighted.

2.3 Studies of Transport and Dispersion Processes

Studies were initiated in the North Dakota program in 1984 to investigate, in more detail, the transport and dispersion of seeding material inside convective clouds. This is an important link in the chain of events hypothesized to lead to modification of the precipitation from such clouds through cloud-base seeding treatments. The experimental approach adopted was the use of SF_6 tracer gas, released from a treatment aircraft, and sampling aircraft equipped with fast-response SF_6 analyzers to follow the transport and dispersion processes in the clouds. Others have also used such techniques to investigate cloud transport processes (e.g., Ching and Alkezweeny, 1986), and similar methods have been employed to study horizontal transport processes on the synoptic scale (e.g., Haagenson *et al.*, 1987). Concurrent release of seeding aerosols along with the SF_6 provides information about the ice-nuclei activation processes.

Key results of the 1984, 1985, and 1987 tracer experiments are summarized in Stith *et al.* (1986, 1990), Stith and Benner (1987), Stith and Politovich (1989), and Huston *et al.* (1991). Zhang (1991) and Stith (1992) discuss some examples of tracer results from the 1989 NDTP. Radar chaff was incorporated as an additional tracer in the NDTP (Martner *et al.*, 1992), and conserved natural trace gases were also used for similar purposes (e.g., Reinking *et al.*, 1992). The latter paper appeared during this contract period, and Appendix F presents a copy of the published abstract. Experiments employing these techniques, plus the use of fluorescent particles as a tracer for identifying hailstone embryo sources (as in Knight *et al.*, 1986), were designed for the North Dakota Tracer Experiment.

2.4 Radar Data Analyses

2.4.1 First-echo analysis

Radar data collected during the 1987 field project by the CHILL S-band radar and during the North Dakota Thunderstorm Project by the NCAR C-band radars CP-3 (Bismarck airport) and CP-4 (near Center) were used in a continuing study of first echoes. Improvements in the Interactive Radar Analysis Software (IRAS) package (see Sec. 2.4.3) now allow the software to run on platforms operating in UNIX. Using the echo history established on the basis of the scans acquired during its lifetime, an investigator can trace an echo backward in time to locate the initial formation. This information is related to the development of precipitation in the clouds.

An M.S. thesis by J. W. Stoppkotte provided a climatological analysis of first echoes from the 1987 and 1989 radar data; a copy of the abstract

of his thesis appears in Appendix G. Figures 2 and 3 summarize the first-echo observations from the respective years; the distribution from 1987 looks quite similar to ones from previous studies in North Dakota (e.g., Koscielski and Dennis, 1976; Miller and Smith, 1986), with a mean first-echo temperature (FET) of -8°C and about a third of the cases having FET > -5°C. The diagram for 1989 is in marked contrast, and presents something of a puzzle; here the mean FET is about -3°C and fully 60% of the values are greater than -5°C. By the usual interpretations, this would suggest a significant warm-rain process in the 1989 clouds, which certainly seems surprising in view of the drought conditions prevailing during the summer project.

The main differences between the radars used in 1987 and 1989 were in wavelength (10 vs. 5 cm, respectively) and overall system sensitivity (the 1989 systems operating with much greater sensitivity). The data used by Koscielski and Dennis and Miller and Smith came from 10 and 5 cm radars, respectively, and no such difference in the FET data appeared there. The difference in sensitivity could be a factor, as detection of weaker initial echoes would usually occur earlier and (in updrafts) at lower altitudes. The first-echo threshold for the 1987 data was generally around 20 dBz, while for the 1989 data, a 10-dBz threshold was usable; this again could lead to earlier first-echo detection at lower heights and higher temperatures. (The issue of first-echo threshold is discussed further in Sec. 2.4.2.) Another complication is that with the priority emphasis placed on the tracer experiments in the 1989 NDTP, the radar scan sequences were less suitable for first-echo census study and so the effective sampling may have differed.

The question of the importance of warm-rain processes in the North Dakota clouds has surfaced in connection with other investigations (e.g., Musil *et al.*, 1993). Stoppkotte presented a synoptic summary for each of the days for which he determined first-echo occurrences and found that on the two days (one in each year) with distinctively lower first-echo heights, a warm front was lying just south of the project area. This would suggest the possibility of an overrunning warm-rain situation. Further indications of this process emerged during the NDTE, in what was certainly not a drought year.

Stoppkotte also looked for correlations between the observed first-echo heights and temperatures and meteorological variables determined from available soundings, or from one-dimensional (1D), steady-state cloud model runs based on those soundings. He found a significant correlation between the daily mean first-echo height (FEH) and the height of the 0°C level. If the two days with the anomalously high FETs are disregarded, the correlation coefficient is 0.83; the regression line lies almost parallel to, and about 1 km above, the 1:1 line. This suggests that temperature is an

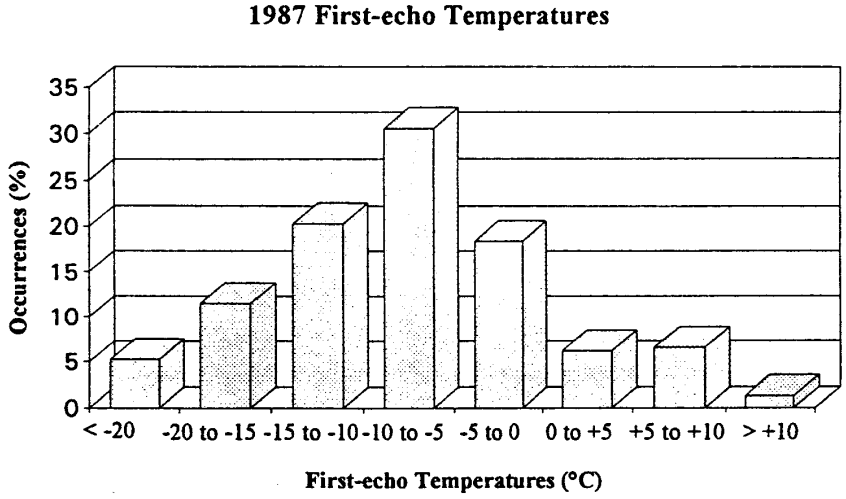

Fig. 2: Histogram of first-echo temperatures for 1987 North Dakota data.

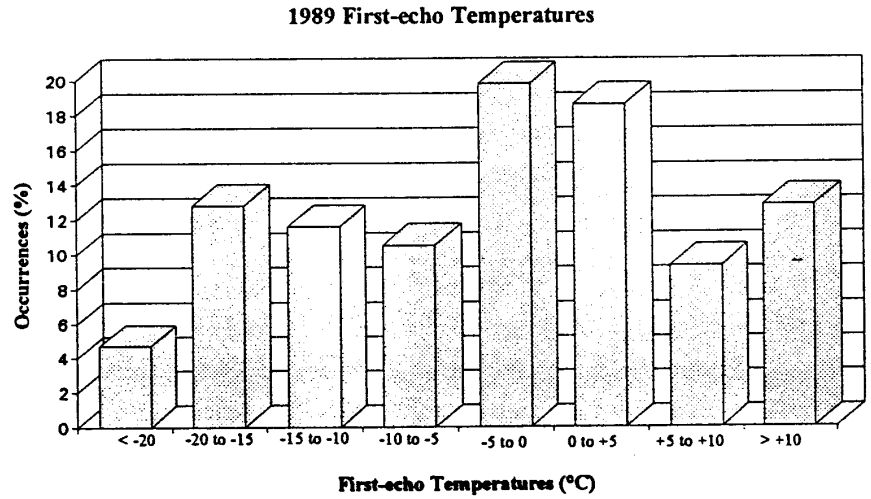

Fig. 3: Histogram of first-echo temperatures for 1989 North Dakota data.

important condition in the development of first echoes in these clouds. Furthermore, using a typical saturated adiabatic lapse rate of 6 degrees per kilometer, this indicates a typical FET of -7°C, which is roughly consistent with a dominant ice process.

Stoppkotte found further significant correlations between some first-echo characteristics (height above cloud base, temperature) and the maximum updraft speeds estimated from a 1D steady-state cloud model based on the nearest available sounding. The effect of updraft strength on first-echo characteristics was recognized at least as early as the work of Battan (1963), and Miller and Smith (1986) provided a relationship for data from the North Dakota area. The Stoppkotte regression line lies almost exactly parallel to the one determined by Miller and Smith, but at about 4°C higher temperatures; the latter may be due in large part to the two days with "warm-rain-type" first-echo characteristics. He also found a correlation coefficient of r = 0.64 between the first-echo height above cloud base and the model-predicted updraft speed, much like that reported by Dennis and Koscielski (1972). Stoppkotte's FEH values were much closer to cloud base than those found by Dennis and Koscielski, but that could be explained by the higher sensitivity of the radar system he used. He found, like they did, no significant correlation between the FET and cloud-base temperature, and also no significant correlation between FET and the in-cloud transport times computed by current versions of the 1D steady-state model. The latter finding raises some questions about the general utility of those transport times in analyses of the tracer experiments (as in Huston *et al.*, 1991).

2.4.2 Thresholds for first-echo determination

Knight and Miller (1990) used the high-sensitivity radars in the NDTP to demonstrate how echo intensities evolve from essentially "clear air" reflectivity values to ones that are characteristic of precipitation. Knight and Miller (1993) further studied this evolution using a polarimetric radar in the Convection and Precipitation/Electrification (CAPE) project. These papers demonstrate that an echo detectable under the right combination of radar sensitivity, range, and cloud characteristics occurs almost simultaneously with the first appearance of visible cloud. This initial echo has a significant, often dominant, Bragg-scattering component that is not related to the development of precipitation in the cloud. The increasing echo intensities that accompany cloud and precipitation formation are thus a continuous process, which brings into question the use of any fixed "first-echo" threshold as an indicator of precipitation initiation.

Previous studies of first-echo characteristics have used a fixed reflectivity threshold, or in many cases just the minimum detectable echo, as an indicator of when and where precipitation is beginning. For such first-echo analyses to have meaning in terms of the initiation of precipitation, it is necessary to establish some threshold of reflectivity to which the initial development of precipitation-sized particles can be related. For example,

Braham and Dungey (1978) suggested a threshold of about 10 dBz to identify the onset of precipitation. Stoppkotte and Smith (1993) re-examined that issue from a microphysical perspective; a copy of their paper appears in Appendix H.

The key results from their paper were derived from Fig. 4, which is based on hypothetical monodisperse droplet-size distributions. Battan (1953) discussed a similar model in connection with first-echo studies, and Plank *et al.* (1955) employed a similar diagram. The first thing apparent from the figure is that particle size is, in general, more important than number concentration in determining the reflectivity factors. For example, raindrops several tenths of a millimeter in diameter, even in fairly low concentrations, would push Z above the range of plausible values for "precipitation-free" cloud conditions. Moving from upper left to lower right across the diagram, an upper limit on the reflectivity for such clouds is set first by the plausible limits on the liquid water concentration (LWC), then by the rainfall rate, and finally by the drop sizes themselves. Above an upper reflectivity boundary near 10 dBz one could assume, with reasonable confidence, that precipitation is present.

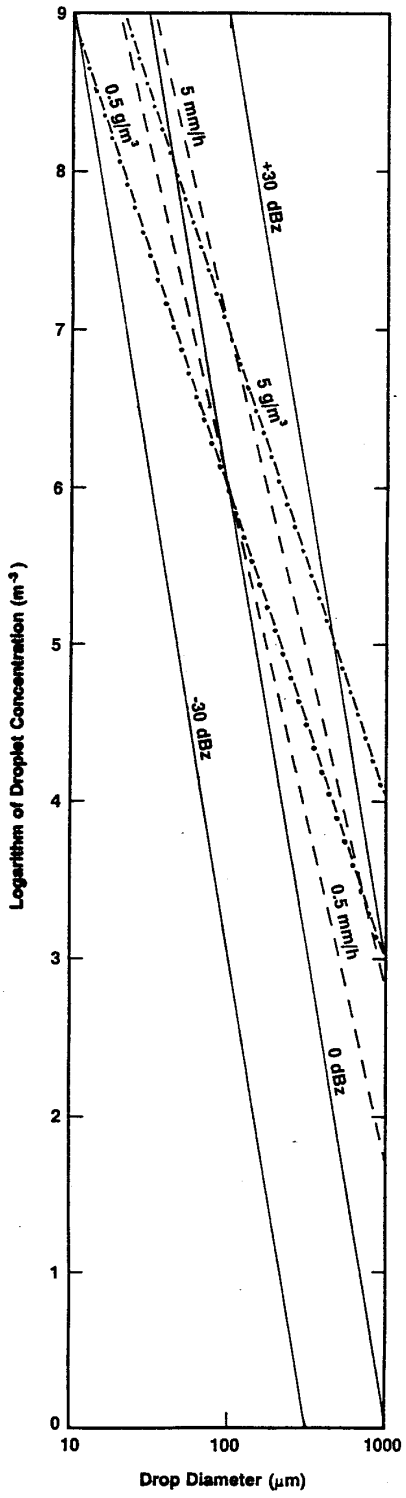

Fig. 4: Diagram relating reflectivity factors to liquid water concentrations and rainfall rates for various monodisperse droplet-size distributions. Solid isolines represent reflectivities; dash-dot lines are LWC's; and dashed lines are rainfall rates.

At the lower end, things are less clear-cut. Drops a few tenths of a millimeter in diameter developing in low concentrations might constitute the onset of precipitation with a considerably lower reflectivity factor. Thus the demarcation between cloud echoes and precipitation echoes in this range of reflectivities is not well defined, and pinpointing the initiation stage becomes quite difficult. This makes the status of census-type studies of first echoes somewhat uncertain.

The growth of particles large enough to produce reflectivities around 0 dBz tends to be quite rapid, so the accompanying rapid increase of Z may reduce the need for concern about an exact threshold for many purposes. If the reflectivity were to pass rapidly from below 0 dBz to above 10 or 15 dBz, then determinations of first-echo heights would depend only weakly on the threshold employed. The question of the effect of first-echo threshold on the observed FEH was explored further using some of the 1989 NDTP radar data. Appendix I gives an edited summary of the study made using computer displays having higher resolution than those available to Stoppkotte. (That elicited some differences which may help to account for the anomalies indicated by Fig. 3.) The basic question examined was whether the FEH is substantially constant over a range of thresholds in the neighborhood of 10 dBz, as might be the case if the echo intensity tends to increase rapidly through this range. Figure 5 indicates that while this is sometimes true (e.g., Echo #11), it does not generally hold.

If the 10-dBz threshold, suggested by Braham and Dungey (1978) and employed in Stoppkotte's analysis of the 1989 data, is used as a reference the echo evolution as summarized in Fig. 6 indicates considerable variation in the observed FEH with the threshold employed. Moreover, no systematic trend of FEH with the threshold reflectivity is apparent. This plot is for first echoes observed at ranges less than 80 km, and the variation in similar plots for cases at longer ranges is somewhat reduced. However, that reflects mainly the increasing vertical extent of the beam with range, so that in the limit only a single height would be identifiable regardless of the threshold used (recall that the basic data involve volume scans at specified elevation steps).

A comparison of the first echoes from each individual day on the same kind of plot did not reveal an obvious pattern that might be associated with the synoptic situation. Consequently, we conclude that the FEH and the corresponding FET vary in an irregular fashion with the reflectivity threshold employed. This makes it more difficult to associate a particular FEH/FET with any particular mechanism of precipitation initiation. The implications of these findings for census-type studies intended to discriminate between hypothesized mechanisms, or to elucidate potential seeding effects, have yet to be established.

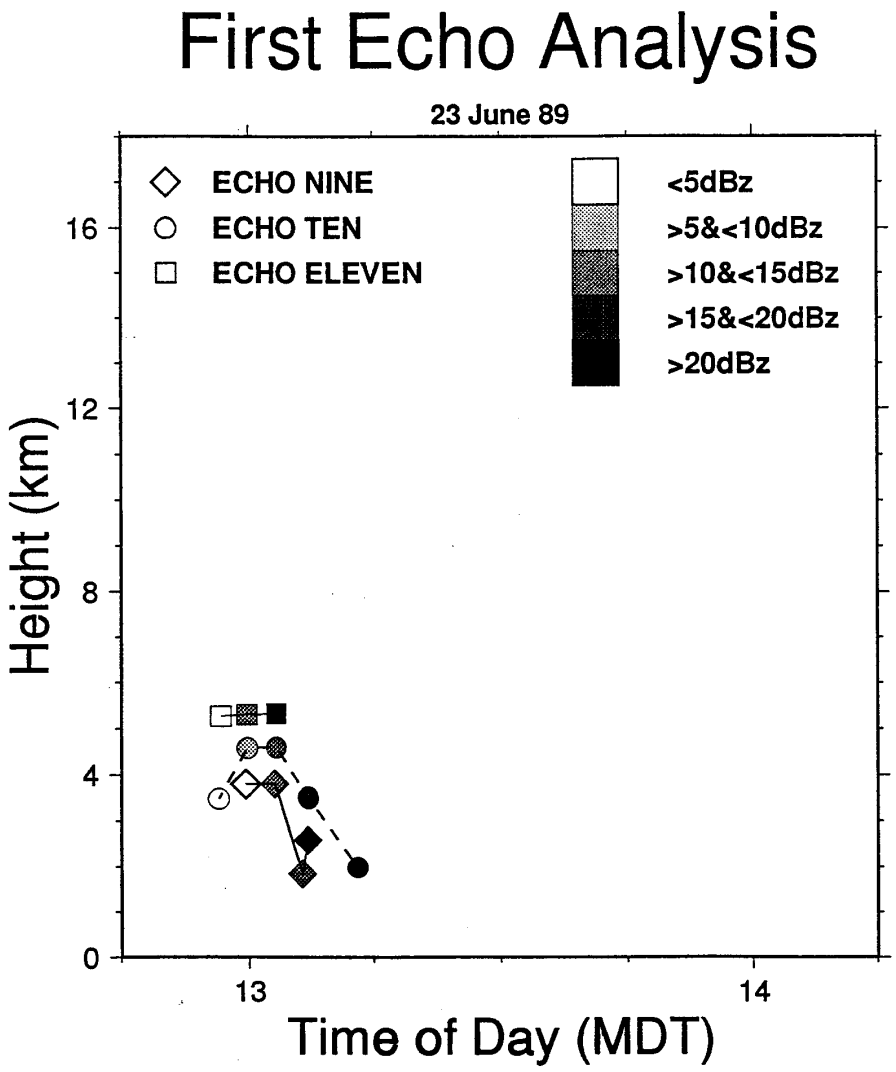

Fig. 5: Example of three "first-echo histories" from 23 June 1989.

2.4.3 Other radar studies

The porting of the Interactive Radar Analysis Software (IRAS) package to UNIX-based workstations was essentially completed during the period. Priegnitz and Hjelmfelt (1993) described the main features of the "Sun IRAS" package as currently available. A copy of that paper appears in Appendix J.

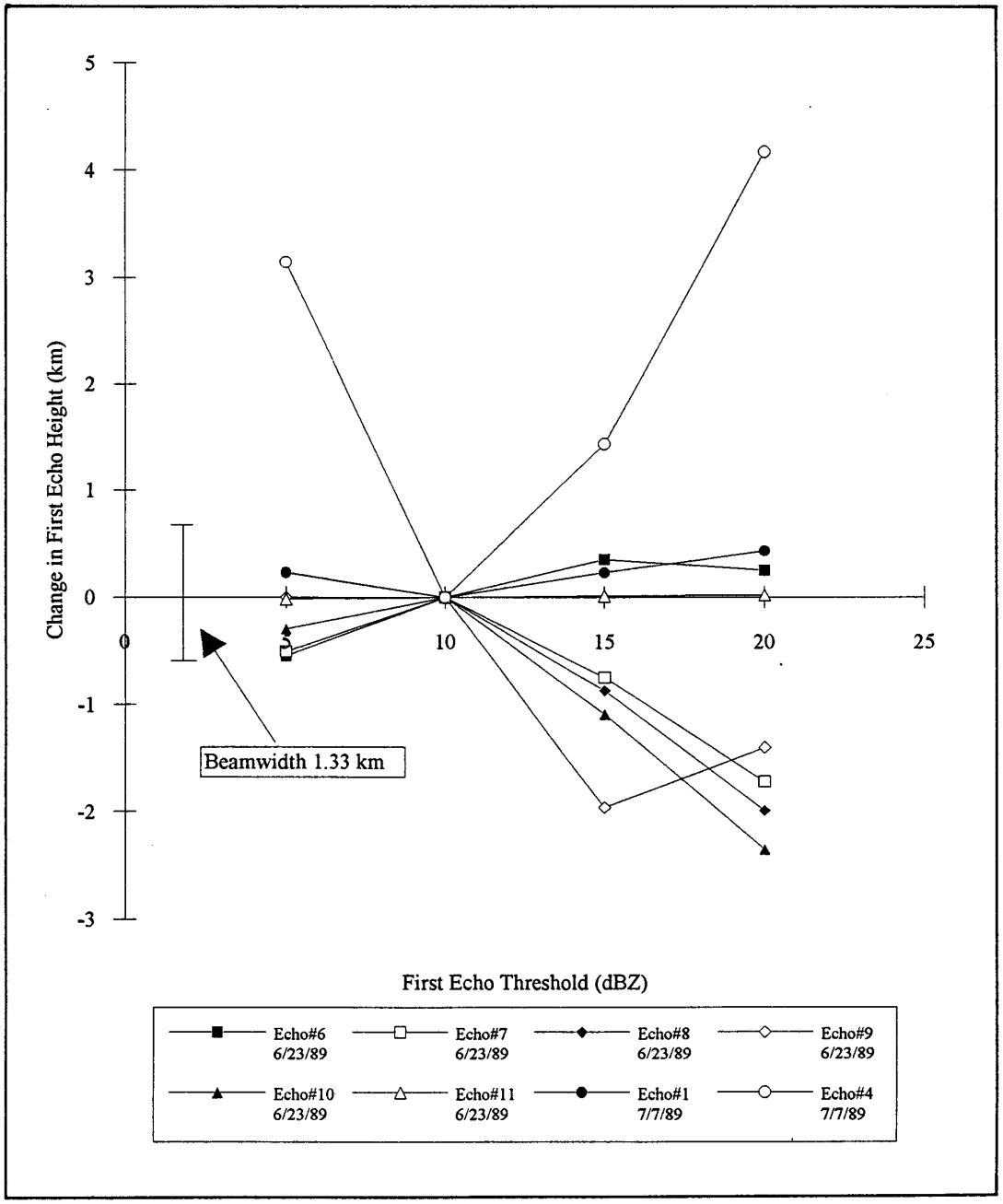

Fig. 6: Effect of reflectivity threshold on first echo height relative to a 10-dBz threshold reference (range < = 80 km).

Maximum echo heights are of interest as indicators of overall storm intensity. Figure 7 shows the distribution of cell maximum echo heights from the NDTP radar observations. The median is about 11 km, which is appreciably higher than the values found in earlier North Dakota studies (e.g. Smith *et al.*, 1985a). That may result partly from the narrower beam-width of the radars used in the NDTP, and also partly from the restricted scanning strategy imposed by the focus on the tracer experiments in 1989. The bimodal nature of the distribution found for 10 July 1989 (Fig. 8) is of some interest in view of the various indications that different air masses influenced the project area during the day (e.g., Musil *et al.*, 1993).

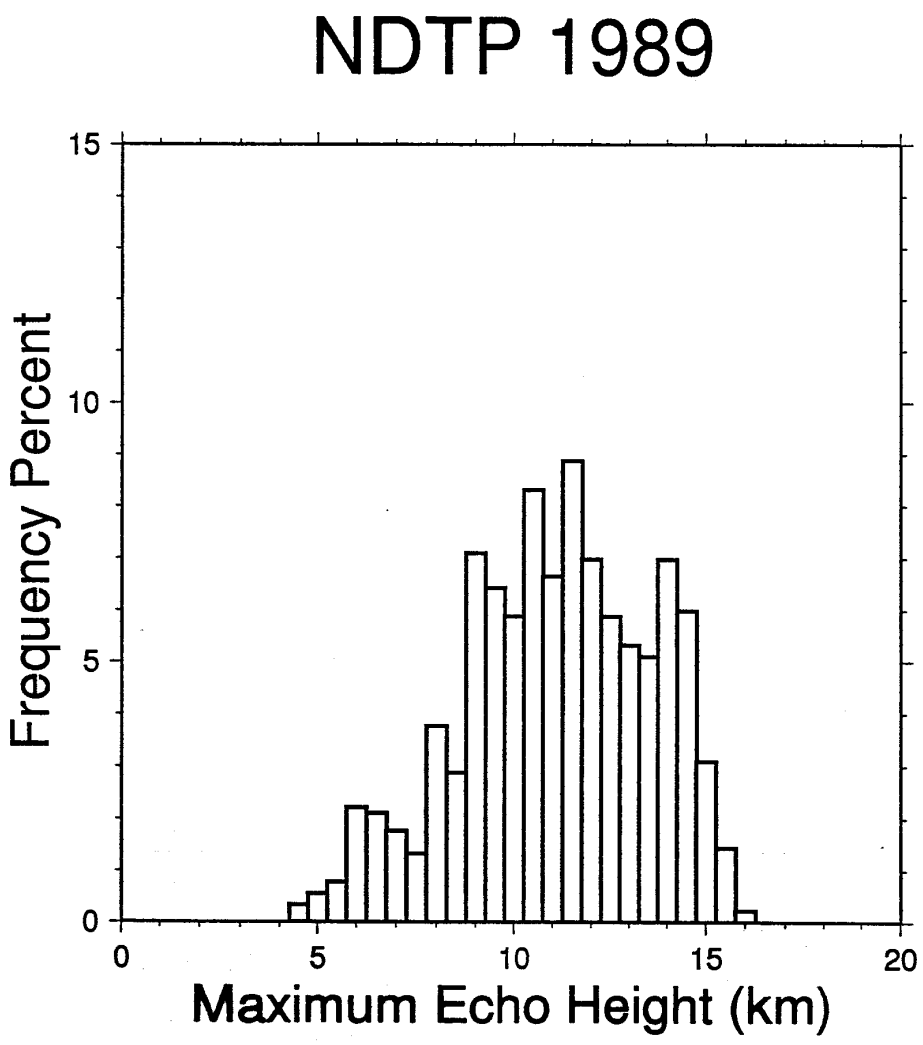

Fig. 7: Frequency distribution of maximum echo heights observed during the NDTP.

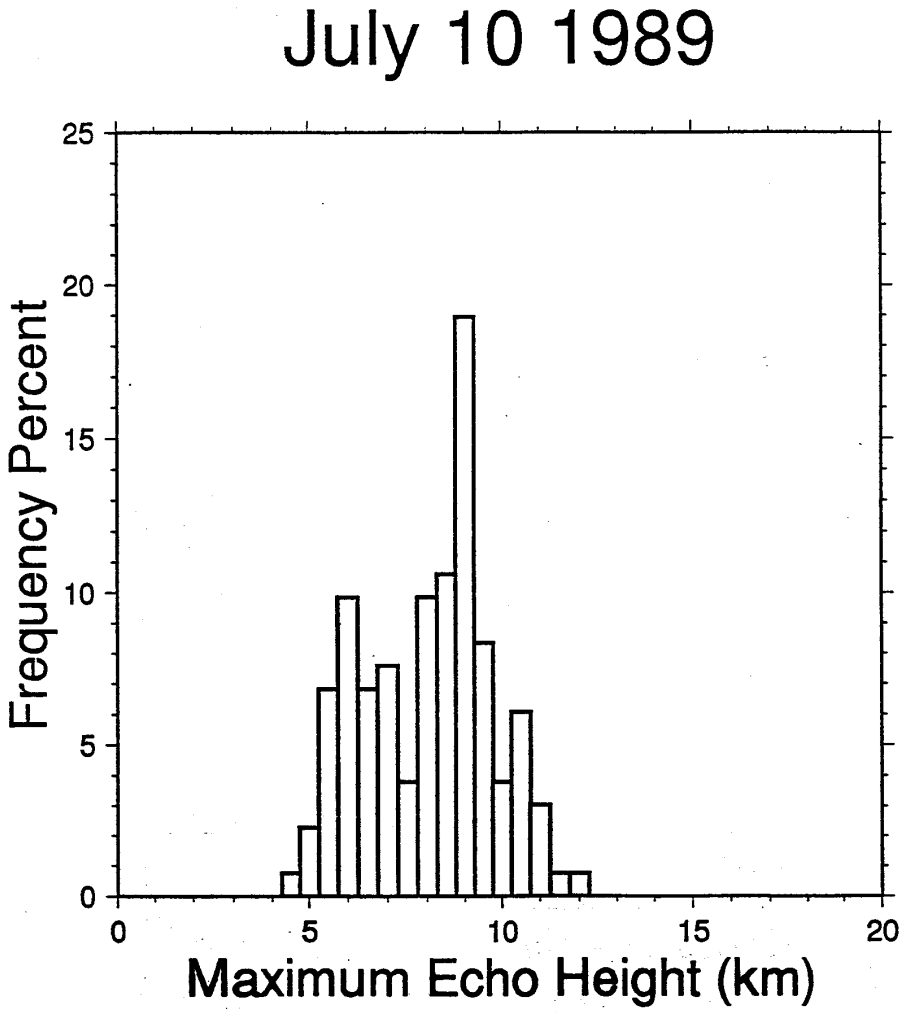

Fig. 8: Frequency distribution of maximum echo heights observed on 10 July 1989.

Recently-revived interest in radar wavelengths shorter than those commonly used in meteorological radars stimulated a review of weather-radar system sensitivity considerations. This included examination of present-day operational and research systems operating at wavelengths from 1.4 mm to 6 m. The basic conclusion, summarized in Smith (1993a,b), was that over the wavelength range from about 1-10 cm, the available system sensitivities are still more or less independent of the wavelength chosen. Attenuation, of course, has increasing effects as the wavelength is decreased below 10 cm, but short-wavelength systems have some advantages for high-resolution studies at short ranges. Appendices K and L present copies of those two papers.

2.5 Numerical Modeling Studies

The manuscript on the application of a two-dimensional, time-dependent numerical cloud model to forecasting, which was submitted some time ago to *Weather and Forecasting*, was revised once again in response to further review comments and has now been accepted for publication. This paper, based on the 1986 COHMEX project and the NDTP, reports on the success of the model's ability to forecast the general convective activity and precipitation potential for a day on the basis of a morning sounding. Appendix M provides a copy of the revised abstract of this paper.

A paper presented at the 13th Conference on Weather Analysis and Forecasting in August contained some of the improvements made in the revised journal article. The National Weather Service (NWS) observations taken during the NDTP were used to sharpen comparisons of the model results with observations. Initially, only subjective observations taken by one of the modelers had been used in evaluating the results; the NWS observations are more quantitative and not made by a potentially-biased observer. The revised assessment of the model performance actually improved to some extent; predictions for precipitation were right 71% of the time, while predictions of cloud development were accurate 85% of the time. A copy of the paper appears in Appendix N.

Simulation of the 28 June 1989 NDTP case is continuing using a three-dimensional (3D), time-dependent cloud model and a 20-size-category hailstorm model. (Most of this work is supported through NSF grants.) Formation of a squall line is captured in the 3D simulation, and growth of hailstones along realistic trajectories is well-illustrated in the 20-category model.

2.6 Extended Wheat-Yield Analysis

The wheat-yield analysis reported in Smith *et al.* (1992d) was extended in a search for information about possible downwind effects. The 17 western North Dakota counties that had been used as a control area were subdivided into two groups. One group (Control 1) consists of eight counties that are almost always upwind of the NDCMP target areas. The second group (Control 2) comprises nine counties that frequently lie downwind from the NDCMP targets.

The statistical analysis procedure was the same as that employed previously. Using Control 1 as a reference, the preliminary results suggest a yield increase in the target areas during the NDCMP years that is quite close to that found previously using the entire control area (about 5-6%).

Moreover, the results indicate a similar (in fact, slightly greater) increase in the downwind Control 2. The implication is that any downwind effects of the NDCMP in this area are at least as favorable as the effects in the target areas themselves. Work to refine this analysis for future publication is under way.

2.7 Planning for the North Dakota Tracer Experiment

Several SDSM&T scientists participated in planning and preparing for the NDTE. Besides the planning meetings in Rapid City and Bismarck, this included work on the draft versions of the field operations plan and arrangements for some of the necessary field facilities. Support of participation in the actual field project was provided mainly under a separate contract.

2.8 Other Activities

An overview of weather modification research activities under the North Dakota component of the Federal/State Cooperative Program and some other related programs was published during the period (Smith *et al.*, 1992a). Appendix O provides a copy of the published abstract.

ACKNOWLEDGMENT

This research was sponsored by the NOAA-North Dakota Cooperative Agreement NA27RA0178-01, Federal-State Cooperative Program in Atmospheric Modification Research under Contract No. ARB-IAS-92-1.

REFERENCES

Battan, L. J., 1953: Observations on the formation and spread of precipitation in convective clouds. *J. Meteor.,* **10**, 311-324.

Battan, L. J., 1963: Relationship between cloud base and initial radar echo. *J. Appl. Meteor.,* **2**, 333-336.

Bluestein, H. B., and M. H. Jain, 1985: Formation of mesoscale lines of precipitation: Severe squall lines in Oklahoma during the spring. *J. Atmos. Sci.*, **42**, 1711-1732.

Boe, B. A., and H. L. Johnson, 1990: Destabilization antecedent to a tornadic northern High Plains mesoscale convective system: A case study. Preprints, *16th Conf. Severe Local Storms,* Kananaskis Park, Alberta, Canada, Amer. Meteor. Soc., 538-541.

Boe, B. A., J. L. Stith, P. L. Smith, J. H. Hirsch, J. H. Helsdon, Jr., A. G. Detwiler, H. D. Orville, B. E. Martner, R. F. Reinking, R. J. Meitin and R. A. Brown, 1992: The North Dakota Thunderstorm Project -- A cooperative study of High Plains thunderstorms. *Bull. Amer. Meteor. Soc.,* **73**, 145-160.

Braham, R. R., Jr., and M. J. Dungey, 1978: A study of urban effects on radar first echoes. *J. Appl. Meteor.,* **17**, 644-654.

Ching, J. K. S., and A. J. Alkezweeny, 1986: Tracer study of vertical exchange by cumulus clouds. *J. Clim. Appl. Meteor.,* **25**, 1702-1711.

Chou, H-Y., 1991: Doppler radar analysis of the 17 July 1989 squall line in North Dakota. M.S. Thesis, Dept. of Meteorology, South Dakota School of Mines and Technology, Rapid City, South Dakota. 88 pp.

Dennis, A. S., and A. Koscielski, 1972: Height and temperature of first echoes in unseeded and seeded convective clouds in South Dakota. *J. Appl. Meteor.,* **11**, 994-1000.

Farley, R. D., T. Wu and H. D. Orville, 1993: Hail production in the 28 June 1989 case. *J. Wea. Modif.,* **25**, 105-114.

Frisch, A. S., B. W. Orr and B. E. Martner, 1992: Doppler radar observations of the development of a boundary layer nocturnal jet. *Mon. Wea. Rev.,* **120**, 3-16.

Haagenson, P. L., Y-H. Kuo, M. Skumanich and N. L. Seaman, 1987: Tracer verification of trajectory models. *J. Climate and Appl. Meteor.,* **26,** 410-426.

Helsdon, J. H., 1990: Analysis of a high positive-flash frequency severe storm (28 June 1989) from the North Dakota Thunderstorm Project. Preprints, *Conf. Atmos. Elec.,* Kananaskis Provincial Park, Alberta, Canada, Amer. Meteor. Soc., 744-745.

Hirsch, J. H., 1989: North Dakota Thunderstorm Project: 1989 Field Program Data Inventory. Bulletin 89-5, Institute of Atmospheric Sciences, S.D. School of Mines and Technology, Rapid City, SD. Dec 1989.

Hjelmfelt, M. R., H-Y. Chou, R. D. Farley and D. L. Priegnitz, 1992: Organization and development of a squall line in North Dakota as revealed by Doppler radar and numerical simulations. Preprints, *5th Conf. Mesoscale Processes,* Atlanta, GA, Amer. Meteor. Soc., 221-226.

Huston, M. W., A. G. Detwiler, F. J. Kopp and J. L. Stith, 1991: Observations and model simulations of transport and precipitation development in a seeded cumulus congestus cloud. *J. Appl. Meteor.,* **30,** 1389-1406.

Johnson, D. B., and M. J. Dungey, 1978: Microphysical interpretation of radar first echoes. Preprints, *18th Conf. on Radar Meteor.,* Atlanta, Amer. Meteor. Soc., 117-120.

Klimowski, B. A., 1993: Initiation and development of rear inflow within the June 28-29 North Dakota meso-convective system. *Mon. Wea. Rev.,* **121.** [In press]

Klimowski, B. A., and J. D. Marwitz, 1990: Single Doppler analyses of a severe squall line and gust front. Preprints, *16th Conf. Severe Local Storms,* Kananaskis Provincial Park, Alberta, Canada, Amer. Meteor. Soc., 252-255.

Klimowski, B. A., and J. D. Marwitz, 1992a: Developing flow structure of a severe squall line. Preprints, *5th Conf. Mesoscale Processes,* Atlanta, GA, Amer. Meteor. Soc., 227-232.

Klimowski, B. A., and J. D. Marwitz, 1992b: The synthetic dual-Doppler analysis technique. *J. Atmos. Oceanic Tech.,* **9,** 728-745.

Knight, C. A., and L. J. Miller, 1990: First 5-cm radar echoes at low dBz values in convective clouds. Preprints, *1990 Conf. Cloud Physics,* San Francisco, CA, Amer. Meteor. Soc., 716-721.

Knight, C. A., and L. J. Miller, 1993: First radar echoes from cumulus clouds. *Bull. Amer. Meteor. Soc.,* **74**, 179-188.

Knight, N. C., A. J. Weinheimer and M. B. Steiner, 1986: The use of powdered iron as a tracer in hailstorm research. Preprints, *Joint Sessions 23rd Conf. Radar Meteor. and Conf. Cloud Physics,* Snowmass, CO, Amer. Meteor. Soc., JP1-JP2.

Koscielski, A., and A. S. Dennis, 1976: Comparison of first radar echoes in seeded and unseeded convective clouds in North Dakota. *J. Appl. Meteor.,* **15**, 309-311.

Martner, B. E., J. D. Marwitz and R. A. Kropfli, 1992: Radar observations of transport and diffusion in clouds and precipitation using TRACIR. *J. Atmos. Oceanic Tech.,* **9**, 226-241.

Miller, J. R., Jr., and P. L. Smith, 1986: Some characteristics of radar first echoes in the High Plains. *J. Wea. Modif.,* **18**, 95-101.

Miller, J. R., Jr., S. Ionescu-Niscov, D. L. Priegnitz, A. A. Doneaud, J. H. Hirsch and P. L. Smith, 1983: Development of physical evaluation techniques for the North Dakota Cloud Modification Project. *J. Wea. Modif.,* **15**, 34-39.

Musil, D. J., A. G. Detwiler, D. L. Priegnitz, M. R. Hjelmfelt and P. L. Smith, 1993: Radar and aircraft investigation of a North Dakota thunderstorm project storm complex (10 July 1989). *Proc. 26th Intnl. Conf. Radar Meteor.,* Norman, OK, Amer. Meteor. Soc., 91-93.

Nair, U. S., 1991: Modeling and observational study of the 28 June 1989 case from the North Dakota Thunderstorm Project. M.S. Thesis, Dept. of Meteorology, S.D. School of Mines and Technology, Rapid City, SD. 144 pp.

Orville, H. D., and N. C. Knight, 1992: An example of a research experience for undergraduates. *Bull. Amer. Meteor. Soc.*, **73**, 161-167.

Orville, H. D., F. J. Kopp, U. S. Nair, J. L. Stith and R. Rinehart, 1990: On the origin of ice in strong convective cells. Preprints, *Conf. Cloud Physics,* San Francisco, CA, Amer. Meteor. Soc., 16-20.

Plank, V. G., D. Atlas and W. H. Paulsen, 1955: The nature and detectability of clouds and precipitation as determined by 1.25-centimeter radar. *J. Meteor.,* **12**, 358-378.

Priegnitz, D. L., and M. R. Hjelmfelt, 1993: Sun-IRAS: An improved package for the display and analysis of weather radar data. Preprints, *26th Intnl. Conf. Radar Meteor.,* Norman, OK, Amer. Meteor. Soc., 335-337.

Reinking, R. F., 1985: An overview of the NOAA Federal-State Cooperative Program in Weather Modification Research. *Proc. 4th WMO Sci. Conf. Wea. Modif.,* Geneva, Switzerland, 643-649.

Reinking, R. F.,1992: The NOAA Federal/State Cooperative Program in Atmospheric Modification Research: A new era in science responsive to regional and national water resources issues. Preprints, *Symposium on Planned and Inadvertent Weather Modification,* Atlanta, GA, Amer. Meteor. Soc., 136-144.

Reinking, R. F., and R. J. Meitin, 1989: Recent progress and needs in obtaining physical evidence for weather modification potentials and effects. *J. Wea. Modif.,* **21**, 85-93.

Reinking, R. F., R. J. Meitin, F. Kopp, H. D. Orville and J. L. Stith, 1992: Fields of motion and transport within a sheared thunderstorm. *Atmos. Res.,* **28**, 197-226.

Rotunno, R., J. B. Klemp and M. L. Weisman, 1988: A theory for strong, long-lived squall lines. *J. Atmos. Sci.*, **45**, 463-485.

Smith, P. L., J. R. Miller, Jr., A. A. Doneaud, J. H. Hirsch, D. L. Priegnitz, P. E. Price, K. J. Tyler and H. D. Orville, 1985a: Research to develop evaluation techniques for operational convective cloud modification projects. Report SDSMT/IAS/R-85/02, Institute of Atmospheric Sciences, S.D. School of Mines and Technology, Rapid City, SD. 93 pp.

Smith, P. L., J. R. Miller, Jr., H. D. Orville, J. H. Hirsch, A. A. Doneaud and D. L. Preignitz, 1985b: Research for physical evaluation of the North Dakota Cloud Modification Project. *Proc. 4th WMO Scientific Conf. Wea. Modif.,* Honolulu, HI, 209-214.

Smith, P. L., H. D. Orville, J. L. Stith, B. A. Boe, D. A. Griffith, M. K. Politovich and R. F. Reinking, 1989: Evaluation studies of the North Dakota Cloud Modification Project. *Proc. 5th WMO Sci. Conf. Wea. Modif. and Applied Cloud Physics,* 8-12 May 1989, Beijing, China.

Smith, P. L., A. G. Detwiler, J. H. Hirsch, L. R. Johnson, F. J. Kopp, J. R. Miller, Jr., H. D. Orville and D. L. Priegnitz, 1990: Development of evaluation techniques for operational convective cloud modification projects: 1988-89 studies. Report SDSMT/IAS/R-90/01, Institute of SDSMT/IAS/R-90/04, Institute of Atmospheric Sciences, S.D. School of Mines and Technology, Rapid City, SD. 24 pp.

Smith, P. L., A. G. Detwiler, J. H. Hirsch, L. R. Johnson, F. J. Kopp, J. R. Miller, Jr., H. D. Orville and D. L. Priegnitz, 1991a: Acquisition and analysis of data for the North Dakota Thunderstorm Project. SDSMT/IAS/R-91/02, Institute of Atmospheric Sciences, S.D. School of Mines and Technology, Rapid City, SD. 22 pp. + app.

Smith, P. L., H. D. Orville and B. A. Boe, 1991b: An overview of the 1989 North Dakota Thunderstorm Project. Preprints, *2nd Yugoslav Conf. Wea. Modif.,* Mavrovo, Yugoslavia, **Vol. I**, 16-24.

Smith, P. L., H. D. Orville, B. A. Boe and J. L. Stith, 1992a: A status report on weather modification research in the Dakotas. *Atmos. Res.,* **28,** 271-298.

Smith, P. L., A. G. Detwiler, J. H. Helsdon, L. R. Johnson, F. J. Kopp, H. D. Orville, D. L. Priegnitz and J. P. Searles, 1992b: Continuing analysis of data for the North Dakota Thunderstorm Project. Report SDSMT/IAS/R-92/01, Institute of Atmospheric Sciences, S.D. School of Mines and Technology, Rapid City, SD. 23 pp. + app.

Smith, P. L., A. G. Detwiler, L. R. Johnson, H. D. Orville and D. L. Priegnitz, 1992c: Further analysis of data from the North Dakota Thunderstorm Project. Report SDSMT/IAS/R-92/07, Institute of Atmospheric Sciences, S.D. School of Mines and Technology, Rapid City, SD. 24 pp. + app.

Smith, P. L., L. R. Johnson, D. L. Priegnitz and P. W. Mielke, Jr., 1992d: A target-control analysis of wheat yield data for the North Dakota Cloud Modification Project region. Preprints, *Symposium on Planned and Inadvertent Wea. Modif.*, 72nd AMS Annual Meeting, Atlanta, GA, 145-147.

Smith, P. L., 1993a: An update on weather radar system sensitivity. *Proc. 26th Intnl. Conf. Radar Meteor.,* Norman, OK., Amer. Meteor. Soc., 384-386.

Smith, P. L., 1993b: Cloud radar system sensitivity versus operating wavelength. *Presented at the GEWEX Topical Workshop on Cloud Profiling Radar,* 29 June-1 July '93, Pasadena, CA.

Stith, J. L., 1992: Observations of cloud top entrainment in cumuli. *J. Atmos. Sci.*, **49**, 1334-1347.

Stith, J. L., and R. L. Benner, 1987: Application of fast response continuous SF_6 analyzer to *in situ* cloud studies. *J. Atmos. Oceanic Tech.,* **4**, 599-612.

Stith, J. L., and M. K. Politovich, 1989: Observation of the effects of entrainment and mixing on the droplet size spectra in a small cumulus. *J. Atmos. Sci.,* **46**, 908-919.

Stith, J. L., D. A. Griffith, R. L. Rose, J. A. Flueck, J. R. Miller, Jr., and P. L. Smith, 1986: A preliminary study of transport, diffusion and ice activation in cumulus clouds using an atmospheric tracer. *J. Clim. Appl. Meteor.,* **25**, 1959-1970.

Stith, J. L., A. G. Detwiler, R. F. Reinking and P. L. Smith, 1990: Investigating transport, mixing and the formation of ice in cumuli with gaseous tracer techniques. *Atmos. Res.*, **25**, 195-216.

Stoppkotte, J. W., and P. L. Smith, 1993: What is a "first echo"? *Proc. 26th Intnl. Conf. Radar Meteor.,* Norman, OK, Amer. Meteor. Soc., 576-578.

Zhang, S., 1991: Two-dimensional model transport simulation in clouds compared with observation. M.S. Thesis, Dept. of Meteorology, S.D. School of Mines and Technology, Rapid City, SD. 74 pp.

Reprinted from the Proceedings of the
11th International Conference on Clouds
and Precipitation, 17-21 Aug 1992, Montreal

APPENDIX A

OBSERVATIONS OF MICROPHYSICAL EVOLUTION IN A HIGH PLAINS THUNDERSTORM

Andrew G. Detwiler and Paul L. Smith
Institute of Atmospheric Sciences
South Dakota School of Mines and Technology
Rapid City, South Dakota, USA 57701

and

Jeffrey L. Stith
Department of Atmospheric Sciences
University of North Dakota
Grand Forks, North Dakota, USA 58202

1. INTRODUCTION

The purpose of this study is to establish the processes within High Plains convective storms that determine the extent and duration of the anvil region. We define the anvil as the elevated part of the cloud that spreads and drifts downshear from the region where deep convection occurs. The ice particles that form the anvil are incompletely-grown precipitation particles and frozen cloud droplets exhausted from this convective region.

The dynamical and microphysical structure of mid-latitude anvil clouds has been studied only recently (*Bennetts and Ouldridge,* 1984; *Heymsfield,* 1986; *Detwiler and Heymsfield,* 1987; *Heymsfield and Miller,* 1988). These clouds have been observed to contain embedded regions of shallow upper-level convection. Particles may grow by deposition in the updrafts in these regions. Aggregation is also a possible growth process (*Heymsfield,* 1986), although aggregates observed in anvils may have formed in the main convective region of the storm and then been transported into the anvil region (*Bennetts and Ouldridge,* 1984). Particle evaporation also occurs, mainly near and below the base of the anvil, and may be accompanied by fragmentation of larger aggregates into smaller ones (*Hallett et al.,* 1989).

Newton (1966) estimated the total water mass transported into the anvil region of one large thunderstorm to be 30% of that which was available for precipitation. *Foote and Fankhauser* (1973) estimated a value of 50% for a storm they studied. *Heymsfield and Miller* (1988) studied six High Plains storms in their mature stages and found the total water mass transport into the anvil to be from 18% to more than 100% of the water vapor mass influx into cloud base (apparently additional water was entrained at mid-levels in at least some cases). There was a good correlation between this percentage and the vertical shear of the horizontal wind, with the lowest percentage corresponding to the smallest shear. The water flux into the anvil was composed of roughly equal proportions of ice and vapor. Ice mass concentration decreased downshear apparently because ice both evaporated, as the anvil mixed with drier environmental air, and precipitated.

Based on these observations, one might expect anvils to be more extensive with increasing vertical shear of the horizontal wind, although no studies have been published demonstrating that such a relationship does indeed exist. It is harder to relate variation in anvil extent to variations in microphysical characteristics of the storm. If the particles entering the anvil were for some reason smaller, or less-heavily rimed and of lower density, then they would be expected to fall more slowly and remain in the upper atmosphere longer. However, smaller particles will evaporate more quickly and dendritic crystals might fragment as they evaporate. There are too few observations of storm anvil microphysics available to find robust correlations between the sizes of particles entering the anvil and storm environmental variables such as windshear, convergence, or vertical stability.

Heymsfield (1986) has described an extensive set of anvil microphysical measurements from a High Plains storm. They were obtained by the NCAR Sabreliner flying in the middle to lower levels of the anvil of the large thunderstorm occurring near Miles City, Montana, on 1 August 1981. His data came from a Particle Measuring Systems (PMS) OAP-2D-P probe. He found that the larger particles ($D > 1$ mm) were predominantly aggregates, and that the size distribution tended to flatten out with distance downshear and downward from the upper region of the storm core -- that is, the proportion of smaller particles decreased and the proportion of larger particles increased. The size of the largest particle observed also increased downshear and downward. He attempted a calculation of particle growth with a kinematic model using Doppler radar wind fields and concluded that aggregation in the anvil was required to explain the large sizes found farther from the core and nearer the base of the anvil.

We contribute here observations of a smaller storm that occurred on 6 July 1989, about 150 km south of Bismarck, North Dakota. The observations were obtained as part of the North Dakota Thunderstorm Project (*Boe et al.,* 1992). *Reinking et al.* (1990, 1992) have discussed the evolution of this storm based on analysis of airborne Doppler radar data and results of a simulation using a two-dimensional, time-dependent cloud model with bulk water microphysics. The focus of the present discussion will be *in situ* microphysical measurements made both in the smaller cumulus congestus clouds forming in the inflow region of the storm by the University of North Dakota Cessna Citation II and the South Dakota School of Mines T-28, and in the upper portions of the anvil by the Citation. Concurrent measurements of ozone concentrations allow an assessment of the potential effects of dilution by entrainment. Although the observations are not sufficient to define all of the processes important to anvil evolution, they do illustrate several interesting features that have not been seen in earlier work.

2. OBSERVATIONS

The storm under study formed late in the afternoon within a dense field of cumulus congestus. It tracked eastward at 20 m/s along the border between North Dakota and South Dakota for several hours. It was in a highly-sheared environment (mainly speed shear, with winds at all levels being predominantly westerly). Cloud base was at 3 km MSL (+4°C temperature) with the tops reaching to 10 km MSL (-40°C), which was slightly below the tropopause height. *Reinking et al.* (1992) describe how the storm was feeding at mid-levels from the south and at low levels from the east. A sketch of the storm based on a recording by the cockpit windscreen video camera in the Citation is shown in Fig. 1, along with schematic locations of aircraft penetrations.

Between 1845 and 1915 CDT (Central Daylight Time), the Citation made several passes over the convective core of the storm at 8.8 km MSL, then back and forth across and along the anvil stretching eastward (downshear) from the core at 8.8 and 9.4 km MSL. At this time, the storm was declining in intensity but was characterized by a high reflectivity core and updraft. Combined aircraft, radar, and model data suggest a single main updraft with maximum speeds between 5 and 15 m/s occurring in the middle and upper levels of the storm during the period of the aircraft observations. An ozone analyzer aboard the aircraft obtained data both in-cloud and during descent outside of cloud; the observations showed that air feeding from mid-levels into the feeders and then into the main updraft of the storm was apparently undergoing little dilution between mid and upper levels of the cloud. Wind fields derived from airborne Doppler radar measurements showed strong divergence at 9 km MSL (*Reinking et al.*, 1992).

The Citation carried a PMS OAP-2D-C probe sampling roughly 5 ℓ/s with an equivalent array height of 1 mm and a resolution of 33 μm. Particles sufficiently large for their features to be distinguished (D > 200 μm) ranged from individual dendritic ice crystals to aggregates, to rimed aggregates, to heavily rimed graupel, much as *Heymsfield* (1986) reported in his observations of the anvil of a somewhat larger High Plains thunderstorm. In addition to the 2D-C, the Citation also carried PMS OAP-1D-C and 1D-P probes. Total particle concentration was several times higher than reported by *Bennetts and Ouldridge* (1984) in the maritime storm they studied, reaching 1000/ℓ near the updraft. This is also more than an order of magnitude higher than concentrations reported in the tops of tropical anvils over Panama by *Knollenberg et al.* (1982). Concentration decreased with distance downshear (north and east) of the convective core. The upper anvil was depleted in larger particles but enriched in smaller particles compared to central levels. The downshear anvil region was depleted in smaller particles and enriched in larger particles compared to the region over the convective core. The largest particles registered by the 1D-P were about 4 mm in diameter and the highest concentrations were found near the upshear region of the storm, within a few kilometers of the updraft.

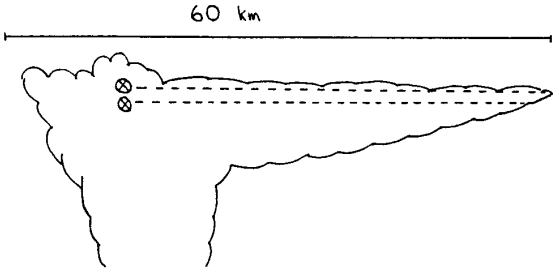

Figure 1: Schematic profile of upper storm as viewed from the south with altitudes of aircraft penetrations indicated by dashed lines.

Figure 2 shows particle size distributions along the northern edge of the anvil based on data from the four PMS probes carried by the Citation. (The high counts in the larger FSSP channels are artifacts due to the presence of high concentrations of ice particles.) Figure 3 shows data from the 2D-C probe, alone, for various regions of the anvil. Highest concentrations are found over the core at 9.4 km, while the largest sizes are downshear at 8.8 km.

There was a trend to more heavily rimed particles nearer the updraft core and lower in the anvil. Also, the particle population was not well mixed; the aircraft would often penetrate small-scale regions (a few hundred meters) with distinct microphysical characteristics, say, high percentages of

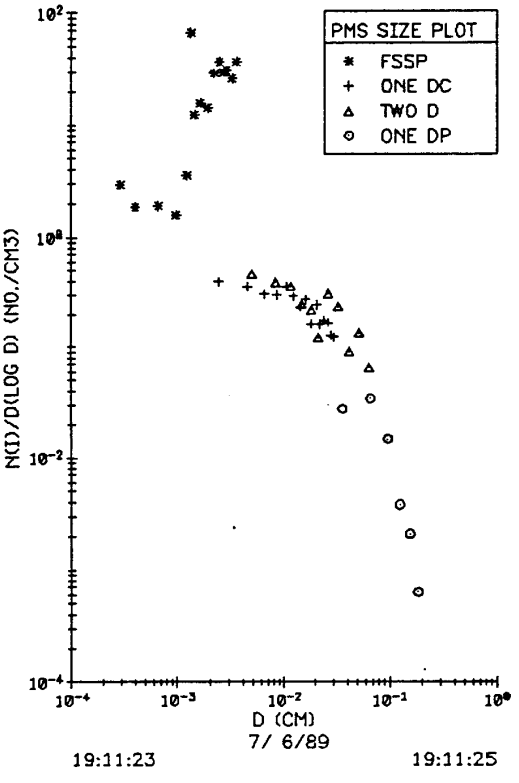

Figure 2: Particle size distribution near north side of anvil, based on the suite of four PMS probes carried by the Citation.

small graupel in one region or large lightly-rimed dendritic snow crystals in another.

Based on ozone and equivalent potential temperature data, the air in the anvil was not strongly diluted by entrainment compared to the air at 8.8 km in the updraft core. Dilution by no more than a factor of two is consistent with measurements made in central regions of the anvil.

T-28 and Citation measurements at 4.5 km (0°C) and 6.5 km (-15°C), respectively, in the convective towers on the south side of the main updraft showed peak cloud droplet concentrations of 500/cm^3. This suggests that also in the main updraft (not penetrated at lower altitudes by either aircraft) droplet concentrations must have been hundreds per cubic centimeter in the 4.5 to 6.5 km altitude range. The maximum 1D-C particle concentration in the anvil over the updraft was about 1/cm^3, and the cloud water concentration was zero (based on a Rosemount icing probe and a Johnson-Williams sensor). The 1D-C can nominally detect particles as small as 15 μm. There could have been a sizable concentration of even smaller particles present, but it is unlikely there were hundreds per cm^3 this small. These 1D-C data give some information concerning the fate of the cloud droplets in the updraft as air rises through the entire depth of the cloud and is "dumped out" of the updraft at the top. If they survive as droplets to approach cloud top regions, they must certainly freeze at some temperature between -35 and -40°C (cloud top temperature was -40°C in this case). If the anvil is characterized by concentrations of 10's to 100's per cubic centimeter of very small ice particles, they must be undetected by the 1D-C. It is more plausible that most of the droplets evaporate or become collected as rime by snow and graupel particles.

The decrease in concentration of smaller particles with distance downshear seen in Fig. 3 argues against an important role for particle breakup during evaporation, at least in the upper regions of the anvil. We lack measurements near the base of the anvil, however, where this mechanism would be more likely to be important.

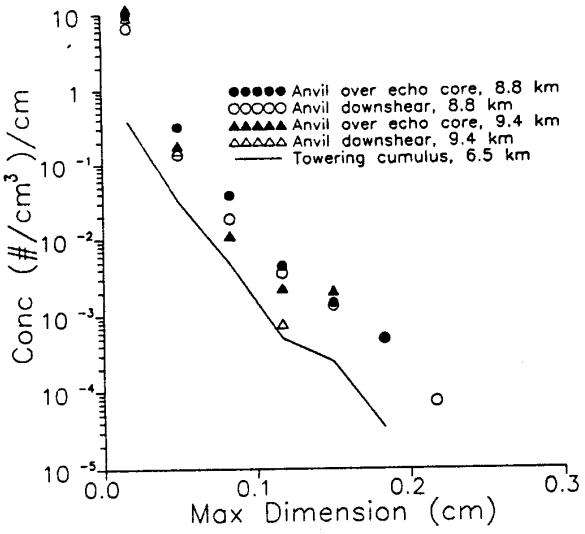

Figure 3: Size distributions from various regions in the anvil based on the Citation 2D-C probe.

One last question we are attempting to address is the relative role in the anvil of aggregation and size-sorting (in size sorting heavier particles don't rise as high and fall out of the anvil more quickly than lighter particles). *Heymsfield* (1986) found evidence for both, but stressed the role of aggregation in producing large aggregates in the lower downshear regions of the anvil from the storm he studied. Here the 2D-C images from 6.5 km altitude in the smaller, neighboring cumulus congestus cells look quite similar to the images obtained in the anvil, although on the average they are not as heavily rimed. (Liquid water concentrations in the smaller clouds are probably much lower than those in the broad updraft of the main storm due to more rapid dilution by entrainment in the smaller updrafts.) Snow particle concentrations are also much lower in the smaller clouds, as shown in Fig 3. It is probable that near the main updraft where the cloud was deeper, higher concentrations of aggregates grew around the 5-15 m/s updraft with ample time to reach large sizes and to rime in the broader region of supercooled water by the time they were carried to near cloud top. The greater breadth of the larger cloud also allows higher concentrations of aggregates to develop over broader regions because entrainment of drier, snow-free air is proportionally less in broader updrafts. *In situ* measurements do show that aggregation in the anvil is not required to explain the presence of 4 mm aggregates there.

It is important to note that our measurements came from the upper portion of the anvil, while Heymsfield's came from the lower portion. It is possible that larger aggregates were present lower in the anvil of this storm.

3. CONCLUSIONS

Airborne *in situ* measurements in the upper regions of the anvil of a strongly-sheared small thunderstorm suggest that most of the mixing between cloud-base air and environmental air occurs while the air is rising in the updraft. Updraft air exhausted into the anvil is only slowly diluted as it drifts off downshear. The anvil is composed of snow particles with a wide range of riming, from nearly spherical graupel to almost pristine spatial forms. The size distribution is steepest (relatively more small particles) near cloud top over the updraft. It flattens and becomes broader at lower altitudes and farther downshear. Number concentration peaks near the upper region near the core of the anvil, where it is several times higher than the concentration reported in the anvil of a small maritime thunderstorm near England and more than 10 times higher than the concentrations found near the tops of tropical anvils near Panama.

The small-ice-particle population is two orders of magnitude smaller in number concentration than the cloud-droplet concentration at mid-levels in the updraft. This fact suggests that almost all of the cloud droplets evaporate or are collected by precipitation particles before they reach the top of the storm, making this storm an efficient processor of cloud water. However, *Reinking et al.* (1992) note that the storm was relatively inefficient at getting precipitation to the ground; more than 50%, and possibly 75%, of the water vapor mass flowing into

the cloud was exhausted into the anvil. The low precipitation efficiency and high particle concentration in the anvil of the storm suggest more and longer-lived anvil cloudiness from this storm compared to maritime anvils like those descibed by Bennetts and Ouldridge.

ACKNOWLEDGMENTS

Support for this research was provided by the National Science Foundation (NSF) under Cooperative Agreements ATM-8620145 and ATM-9104474; NSF Grant No. ATM-8720252; the NOAA Federal/State Cooperative Program under agreements NA 900AA-H-0A176 and NA 17RA0218-01 and via North Dakota Atmospheric Resource Board Contracts NDARB-UND-NOAA90 and NDARB-UND-NOAA91.

REFERENCES

Bennetts, D. A., and M. Ouldridge, 1984: An observational study of the anvil of a winter maritime cumulonimbus cloud. *Quart. J. Roy. Meteor. Soc.*, **110**, 85-103.

Boe, B. A., J. L. Stith, P. L. Smith, J. H. Hirsch, J. H. Helsdon, Jr., A. G. Detwiler, H. D. Orville, B. E. Martner, R. F. Reinking, R. J. Meitin and R. A. Brown, 1992: The North Dakota Thunderstorm Project: A cooperative study of High Plains Thunderstorms. *Bull. Amer. Meteor. Soc.*, **73**, 145-160.

Detwiler, A., and A. J. Heymsfield, 1987: Air motion characteristics in the anvil of a severe thunderstorm during CCOPE. *J. Atmos. Sci.*, **44**, 1899-1911.

Foote, G. B., and J. C. Fankhauser, 1973: Airflow and moisture budget beneath a northeast Colorado hailstorm. *J. Appl. Meteor.*, **12**, 1330-1353.

Hallett, J., S. Ahmed, Y. Y. Dong and R. G. Oraltay, 1989: Secondary ice crystal production in the atmosphere: Its role in assessment of cloud seeding effectiveness. Preprints, *5th WMO Conf. Wea. Modif. and Appl. Cloud Physics,* Beijing, China. WMO/TD - No. 269, WMO Secretariat, Geneva, Switzerland, 43-46.

Heymsfield, A. J., 1986: Ice particle evolution in the anvil of a severe thunderstorm during CCOPE. *J. Atmos. Sci.*, **21**, 2463-2478.

Heymsfield, A. J., and K. M. Miller, 1988: Water vapor and ice mass transported into anvils of CCOPE thunderstorms: Comparison with storm influx and rainout. *J. Atmos. Sci.*, **22**, 3501-3514.

Knollenberg, R. G., A. J. Dascher and D. Huffman, 1982: Measurements of the aerosol and ice crystal populations in tropical stratospheric cumulonimbus clouds. *Geophys. Res. Letters,* **9**, 613-616.

Newton, C. W., 1966: Circulations in large sheared cumulonimbus. *Tellus,* **18**, 699-713.

Reinking, R. F., R. J. Meitin, F. Kopp, H. D. Orville and J. L. Stith, 1992: Fields of motion and transport within a sheared thunderstorm. *Atmos. Res.* [In press]

Reinking, R. F., J. L. Stith and R. J. Meitin, 1990: Airborne Doppler radar and *in situ* studies of the transport of ozone and other constituents in feeder cells and anvils. Preprints, *1990 Conf Cloud Physics,* San Francisco, Amer. Meteor. Soc., Boston, MA, 698-705.

APPENDIX B

ICE-PRODUCING PROCESSES IN NORTH DAKOTA CLOUDS

Andrew G. Detwiler and Paul L. Smith
South Dakota School of Mines and Technology
Rapid City, South Dakota 57701 USA

Jeffrey L. Stith
University of North Dakota
Grand Forks, North Dakota 58202 USA

1. INTRODUCTION

First-echo studies of clouds in the northern US High Plains generally support the hypothesis that the ice process is the dominant mechanism by which precipitation typically forms, although some studies do show a significant percentage of "warm" first echoes (e.g., *Miller and Smith,* 1986; *Dennis and Koscielski,* 1972; *Koscielski and Dennis,* 1976) We present here observations of a convective cloud examined by aircraft, ground-based photography, and radar during a recent field experiment, the North Dakota Thunderstorm Project (NDTP), organized under the NOAA Federal-State Cooperative Program in Atmospheric Modification Research (*Boe et al.,* 1992). This cloud evolved very quickly. We show how the development of the first echo in this cloud compares to earlier first echo studies, and also show where ice particle growth first began in the cloud.

2. OBSERVATIONS

Late in the day on 27 June 1989, a complex of thunderstorms moved within range of NDTP radars from the south-southwest. *Meitin and Brown* (1990) have discussed some of the features of the evolution of this storm. At 2015 CDT (Central Daylight Time), (hereafter designated t_0), a small towering cumulus cloud developed out of the leading edge of pre-existing cloud upwind of one of a pair of mature thunderstorms, in the manner of a daughter cloud, or new cell in a propagating chain of thunderstorm cells. This tower grew explosively from 7 km to almost 10 km MSL within 7 min as it propagated downshear above lower cloud debris. It was apparently in an environment not conducive to sustained development, and was collapsing by 2032 CDT, the time of the last available photograph. Figure 1 shows a time history of the cloud top profile based on photographs from a site some 84 km to the north.

A sector volume scan by a C-band radar with a 1 deg beamwidth situated 57 km to the northeast beginning at 2019 CDT (t_0 + 4 min) showed a small region of -2 dBz echo at 6 km MSL (where the temperature was -13°C) in this cell. The School of Mines T-28 research aircraft penetrated this same region at 6 km MSL at 2024 CDT (t_0 + 9 min). At this time, the visible cloud top was at 9.5 km (-40°C) and had been rising at about 15 m/s over the 3 min prior to this penetration. An echo of 4 dBz was detected at 8 km (-28°C) and at 4 km (0°C) in this region, but no

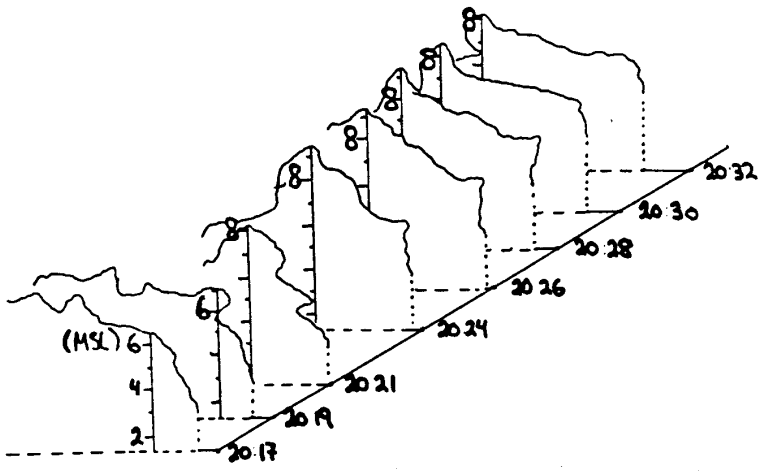

Figure 1: Profiles of cloud top based on photographs taken from 84 km north. Baseline labeled with times represents the 183° azimuth from the photographer. Height scales in km.

echo above -8 dBz was detected at the penetration altitude at this time. The aircraft found updrafts of about 10 m/s and cloud liquid water concentrations of 0.67 g/m^3 at 6 km. The two-dimensional optical array imaging probe (a Particle Measuring Systems OAP-2D-C) on the aircraft detected small ice particles (maximum dimension less than 500 μm) with a peak concentration of about 1/ℓ.

A second minimally-instrumented project aircraft penetrating at 4 km MSL (0°C) found peak liquid water concentrations of 2.3 g/m^3. This aircraft noted strong updrafts but obtained no quantitative measure of them, nor was it capable of recording precipitation particles. Thus, radar, photographic, and *in situ* evidence at this time show the cloud to be vigorously growing.

The T-28 re-penetrated the tower two more times at 6 km and one final time at 5.7 km, at 20:28:30 (t_0 + 13:30), 20:34:30 (t_0 + 19:30) and 20:38:15 (t_0 + 23:15), respectively, finding mostly downdrafts in the cloud. No measurable deviation of electric fields from fair weather values was found (to within 100 V/m). As the precipitation initiated aloft fell through the aircraft altitude, the 2D-C probe showed it to be composed of concentrations up to 3/ℓ of graupel, reaching sizes as large as 2 mm on the 3rd penetration (t_0 + 19:30), but only as large as 1 mm on the final penetration (t_0 + 23:15). (See Fig. 2.) Peak cloud water concentrations were again 0.67 g/m^3 on the second pass, but only about 0.10 g/m^3 on the 3rd and 4th passes as the cloud collapsed. Maximum reflectivity at aircraft penetration locations in the final two penetrations was about 10 dBz (radar coverage was absent during the second T-28 penetration).

3. ANALYSIS

Observations described above show that, although this cloud did not develop into a mature thunderstorm, precipitation did form aloft within

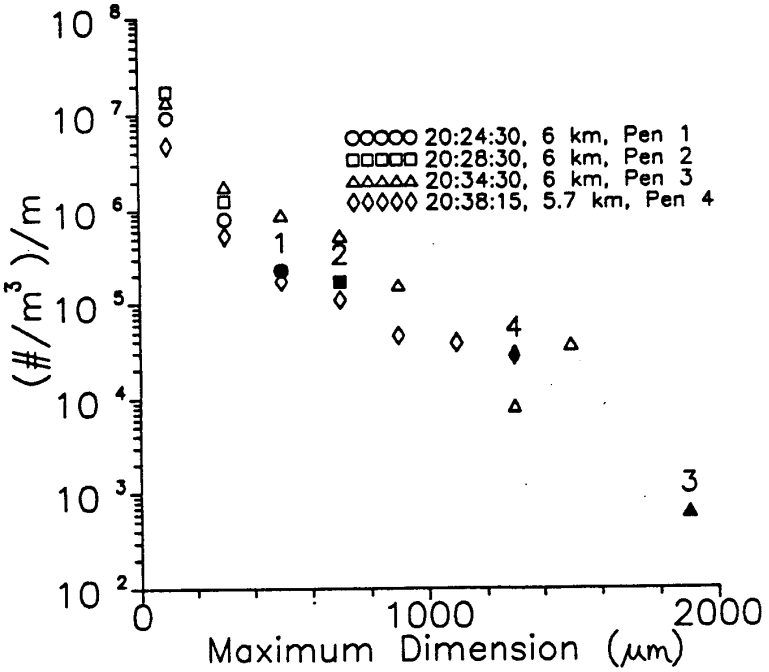

Figure 2: Particle size distributions for each of 4 tower penetrations by T-28. Filled symbols represent largest size observed on respective penetrations.

it in the manner expected for a High Plains cumulus. The first radar echo (-2 dBz) appeared at the -13°C level during a period of explosive growth with cloud top rising at about 15 m/s. Based on laboratory experiments reported in *Scorer* (1957), one might infer a peak updraft in the cloud of approximately twice the rate of rise of the top, or 30 m/s, during the period leading up to the first T-28 penetration (although only 10 m/s was measured at 6 km). Visible cloud existed in the region from which the tower grew, and cloud-top temperatures there were about -20°C, but there was no radar echo within or beneath the growing tower exceeding -6 dBz as the tower began to grow. Four minutes after the first echo appeared at the 6 km level, the maximum echo observed in the tower was in two pockets of 4 dBz, one at an altitude of 8 km (-28°C) and the other at 4 km (0°C). It was determined that the upper echo was due to low concentrations of graupel that were millimeter-size (at least by the time they fell through the 6 km level). The origin of the lower echo is not known.

The appearance of first echo greater than 0 dBz at two heights simultaneously, and the phenomenon reported by *Knight et al.* (1983) of first echo appearing simultaneously over a continuous altitude range spanning several kilometers, point to some of the problems in interpreting first-echo observations in terms of a simple conceptual single-updraft cloud model. Our observations do suggest that ice began growing at temperatures at least as high as -13°C, as evidenced by the -2 dBz echo and ice

particles found at this temperature as the cloud was beginning its growth particles suggests this to represent the onset of significant precipitation. The fact that this tower grew upwind of pre-existing cloud with top temperatures as low as -20°C introduces ambiguity in determining where and at what temperature natural ice nucleation first occurred at significant rates, but the observations are consistent with natural ice nucleation beginning at temperatures higher than -13°C.

4. CONCLUSIONS

Radar, aircraft, and photographic observations of a short-lived cumulus tower are used to investigate some aspects of ice nucleation and precipitation development in the cloud. Natural ice nucleation may have begun at temperatures higher than -13°C, but significant precipitation growth did not occur until lifting of several kilometers had occurred.

ACKNOWLEDGMENTS

We appreciate the cooperation of all NDTP participants, but particularly Charles Knight in collecting the data for this study. Support from NOAA Federal/State Cooperative Agreement NA90AA-H-OA176, Federal State Cooperative Program in Atmospheric Modification Research under Contracts No. ARB-IAS-89-1 and ARB-IAS-91-2, NSF Cooperative Agreements ATM-8620145, ATM-9104474, and Grant No. ATM-8720252 is gratefully acknowledged.

REFERENCES

Boe, B. A., J. L. Stith, P. L. Smith, J. H. Hirsch, J. H. Helsdon, Jr., A. G. Detwiler, H. D. Orville, B. E. Martner, R. F. Reinking, R. J. Meitin and R. A. Brown, 1992: The North Dakota Thunderstorm Project: A cooperative study of High Plains thunderstorms. *Bull. Amer. Meteor. Soc.*, **73**, 145-160.

Dennis, A. S., and A. Koscielski, 1972: Height and temperature of first echoes in unseeded and seeded convective clouds in South Dakota. *J. Appl. Meteor.*, **11**, 994-1000.

Knight, C. A., W. D. Hall and P. M. Roskowski, 1983: Visible cloud histories related to first radar echo formation in northeast Colorado cumulus. *J. Clim. Appl. Meteor.*, **22**, 1022-1040.

Koscielski, A., and A. S. Dennis, 1976: Comparison of first radar echoes in seeded and unseeded convective clouds in North Dakota. *J. Appl. Meteor.*, **15**, 309-311.

Meitin, R. J., and R. A. Brown, 1990: A dual-Doppler analysis of North Dakota thunderstorms using airborne and ground-based radars. Preprints, *16th Conf. Severe Local Storm*, Kananaskis Provincial Park, Alberta, Canada. Amer. Meteor. Soc., 225-230.

Miller, J. R., Jr., and P. L. Smith, 1986: Some characteristics of radar first echoes in the High Plains. *J. Wea. Mod.*, **18**, 95-101.

Scorer, R. S., 1957: Experiments on convection of isolated masses of buoyant fluid. *J. Fluid Mech.*, **2**, 583-594.

APPENDIX C

OBSERVATIONS OF MICROPHYSICAL EVOLUTION IN A HIGH PLAINS THUNDERSTORM ANVIL

Andrew G. Detwiler,[a] Paul L. Smith,[a]
Jeffrey L. Stith[b] and Donald A. Burrows[b]

[a]*Institute of Atmospheric Sciences, South Dakota School of Mines and Technology, Rapid City, South Dakota 57701, USA*

[b]*Department of Atmospheric Sciences, University of North Dakota, Grand Forks, North Dakota 58202, USA*

ABSTRACT

An instrumented aircraft performed several penetrations of the upper regions of a High Plains thunderstorm anvil. The concentrations of particles larger than about 50 μm were up to 10^6 m^{-3}, which is much higher than has been found in some other studies of the anvil regions of thunderstorms. The spatial variation of microphysical population characteristics in the upper regions of the anvil is consistent with a size-sorting process and aggregation within the anvil region.

APPENDIX D

ICE-PRODUCING PROCESSES IN A NORTH DAKOTA CUMULUS CLOUD

Andrew G. Detwiler,[a] Paul L. Smith,[a] Jeffrey L. Stith[b]
and Donald A. Burrows[b]

[a]*Institute of Atmospheric Sciences*
South Dakota School of Mines and Technology
Rapid City, South Dakota 57701 USA

[b]*Department of Atmospheric Sciences*
University of North Dakota
Grand Forks, North Dakota 58202 USA

ABSTRACT

The early development of ice particles in a convective cloud is monitored using radar and instrumented aircraft. Observed ice particle concentrations (~1000 m^{-3}) at the -13°C level in updraft regions are consistent with recent surveys of ice nuclei concentrations but are high compared to earlier surveys. An adiabatic parcel model with an ice nucleation parameterization based on the more recent surveys produces an initial ice particle population at the -13°C level that closely resembles that observed. The observations suggest that in this cloud ice particles first nucleated in the air rising in the updraft region below this level. These particles began to grow to precipitation sizes just as the updraft began to collapse. Due to lack of supercooled cloud water, ice particles that nucleated later at higher and colder levels did not grow to precipitation sizes. Maximum concentrations of small graupel particles reached only 2×10^4 m^{-3} near the -10°C level in the cloud even though cloud-top temperatures as low as -40°C were attained.

Reprinted from the preprint volume of the 26th International Conference on Radar Meteorology, 24-28 May 1993, Norman, OK. Published by the American Meteorological Society, Boston, MA

3.10

APPENDIX E

RADAR AND AIRCRAFT INVESTIGATION OF A NORTH DAKOTA THUNDERSTORM PROJECT STORM COMPLEX (10 JULY 1989)

Dennis J. Musil, Andrew G. Detwiler, David L. Priegnitz,
Mark R. Hjelmfelt, and Paul L. Smith

Institute of Atmospheric Sciences
South Dakota School of Mines and Technology
Rapid City, South Dakota 57701-3995

1. INTRODUCTION

A large mass of thunderstorms moved into the North Dakota Thunderstorm Project (NDTP) operating area (Boe *et al.,* 1992) from western North Dakota during the mid-afternoon of 10 July 1989. These storms and the cells embedded within them moved rapidly toward the northeast at speeds near 22 m/s. This paper describes microphysical and electric field measurements made by the armored T-28 aircraft, and their relationship to radar observations of the storms.

The cloud-base temperature on this day was about +9°C. Radar observations near the time of the T-28 penetrations showed a large convective complex with numerous embedded storms. One storm (A in Fig. 1), identifiable in various stages of development between 2000 and 2130 CDT, was penetrated six times. The penetrations occurred in three pairs, at nominal temperatures of -11, -8, and -3°C, respectively. While descending through the melting level on its return to Bismarck, the T-28 penetrated a line of smaller clouds (Fig. 1, bottom) which probably formed on an outflow boundary associated with the larger cloud mass to the northwest.

The acquisition of *in-situ* data at different levels in the same storm of a persistent weak multicell complex (in which storm the strongest reflectivities remained below the 0°C level, Fig. 2) makes this case of interest. The observations of hydrometeors in conjunction with electric field data provide possible corroboration of various theories of charge separation, as well as clues regarding the precipitation mechanism. The single penetration of the line provides information on hydrometeors near the melting level in a different type of storm.

2. STORM A

The six penetrations (Table 1) were characterized by moderate updrafts with maxima <10 m/s. Cloud LWC values were relatively low

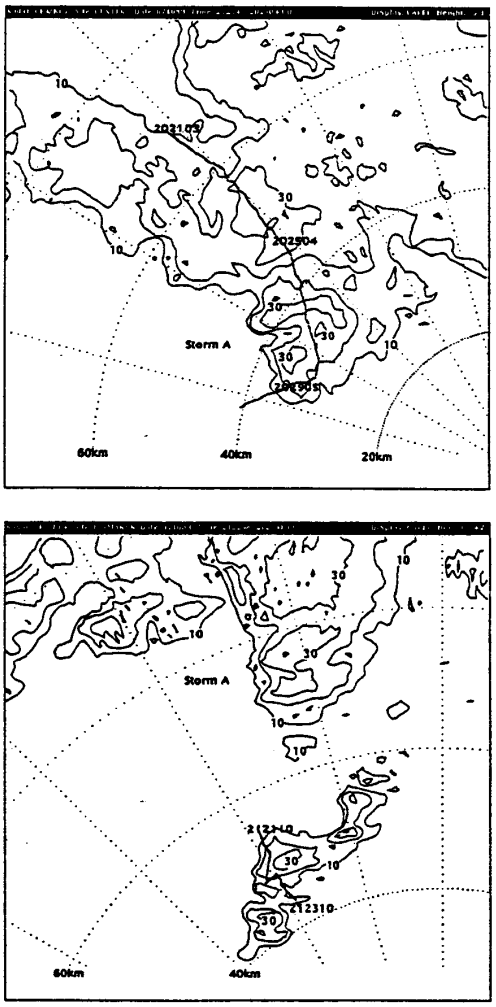

Fig. 1: CAPPI plots near T-28 altitudes for Penetrations 2 (top) and 7 (bottom). Contours start at 10 dBz with a contour interval of 10 dB. The T-28 flight track is indicated.

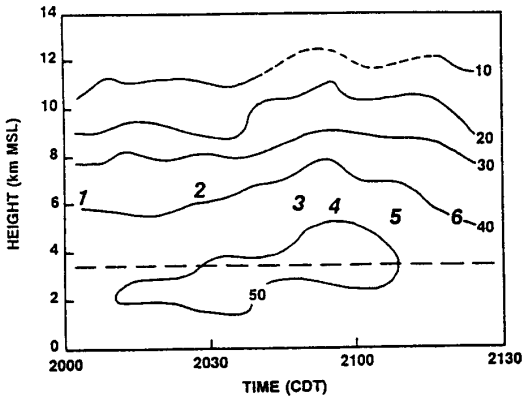

Fig. 2: Time-height reflectivity cross section of Storm A during the period of the T-28 penetrations. Contours are in dBz, and bold numbers represent approximate times and altitudes of T-28 penetrations. Horizontal line indicates cloud base.

TABLE 1: Averages of Conditions in Storm A

Pen	T (°C)	Start (CDT)	Distance (km)	Vertical Field* (kV/m)	Vertical Wind (m/s)	Hail Conc (m^{-3})	Shadow-Or Conc* (ℓ^{-1})
1	-11	200300	4.5	-14	-2.4	0	150
2	-11	202600	16.2	-30	0.7	0.1	500
3	-8	204645	5.8	-7	0.6	0	120
		204750	2.7	+3	2.3	3.1	170
		204821	3.5	-12	1.7	0.7+	240
4	-8	205445	8.9	-23	-0.9	0.7+	460
		205625	4.5	+7	4.3	2.4	140
5	-3	210715	3.5	-5	2.3	3.1	70
6	-3	211300	11.7	+17	0.8	2.3	160

*1-km average around highest values.
+Hail mostly near edge of adjacent positive-field region.

(generally <1 g/m^3). Moderately high concentrations of particles (predominantly, if not exclusively, ice) were observed with a PMS 2D-C probe, and hail was present in small sizes and amounts in several regions.

The time-height cross section of the reflectivity structure of Storm A in Fig. 2 indicates the approximate time and altitude of each T-28 penetration. The T-28 encountered reflectivities exceeding 30 dBz much of the time. The strongest reflectivity was found below 5 km throughout the flight (the 0°C level was at 4.6 km) and exceeded 50 dBz for about an hour. The maximum reflectivity decreased with height, above this level; the absence of reflectivity maxima aloft is an unusual feature of this storm. The weak to moderate updrafts present in this storm and the reflectivity structure suggest a precipitation mechanism where the hydrometeors continued to grow during their descent through the cloud. The observed ice-particle concentrations showed some tendency toward lower values at lower altitudes, which could indicate an aggregation process.

The 2D-C probe data also showed a wide variety of ice particle habits (Fig. 3). Many of the particles were rounded but there were substantial numbers of irregular particles, mainly graupel, aggregates, rimed snowflakes, and a few columns. The round particles looked like rough graupel, especially at the lower temperatures; however, they were only slightly smoother in appearance during the warmer penetrations. The hail sensor also observed large particles, probably ice. Thus, the particles (larger than about 100 μm) found in Storm A were almost exclusively ice between temperatures of -11 to -3°C.

The observations in Storm A were separated according to sign for variables that might provide clues about charge separation (Table 1). In most cases, the electric fields were negative, with weak updrafts or downdrafts and little hail. The three positive-field regions, which indicate negative charge above and/or positive charge below the aircraft, were also characterized by weak updrafts but had high concentrations of hail particles. This contrasts with Detwiler *et al.* (1990), who observed negative fields when the hail particles were present. Penetration 5 was an exception, but it had the weakest negative field found in Storm A. The 2D-C Shadow-Or concentrations (indicative of small ice particles) were highest in the regions with strong negative fields.

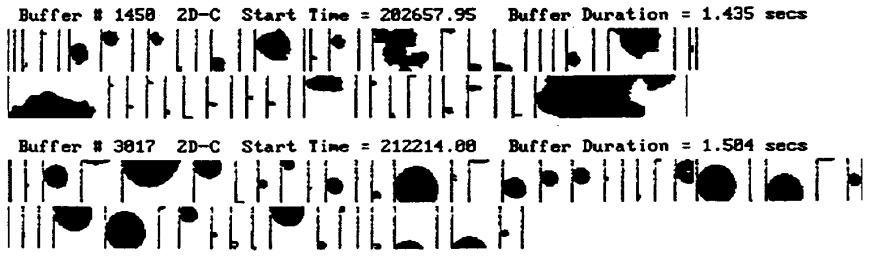

Fig. 3: Sample images from 2D-C probe for Penetration 2 near -11°C (upper) and Penetration 7 near 0°C (lower). Vertical bars represent about 1 mm.

3. ECHO LINE

The line penetrated on the T-28's return to Bismarck had two phases: an initiation/expansion phase between about 2000-2045 CDT, followed by the development of the line itself. Small clouds first appeared a few km southeast of the main echo mass, and the initial echo appeared around 2015. The mode of growth showed new cumulus development near the southwest corner of the cloud, which evolved into a contiguous echo. The clouds steadily sheared off to the northeast while they grew. The strongest reflectivities appeared to develop around 3.5 km altitude (well below the melting level) and spread vertically in both directions, similar to the behavior of Storm A. The reflectivity reached slightly over 40 dBz during the expansion phase. Cloud tops were about 7 km, substantially lower than the top associated with Storm A.

About 2045 CDT, the echoes became loosely arranged in a northeast-southwest line about 40-50 km long and 10-15 km wide. The line intensified around 2100 and afterwards had several cells present simultaneously; maximum reflectivities remained around the 3.5 km level and increased to >50 dBz at times. New development continued to appear near the original initiation point with a structure similar to that prior to the line phase. The T-28 penetration (No. 7) at about 2122 was transverse to the line and passed through one of the cells present at that time (see Fig. 1). The aircraft was descending through the melting level, beginning near a temperature of -2°C and ending at about +2°C upon exit from the line.

The most striking feature of the particles encountered was the smooth round nature of the 2D-C images (Fig. 3), apparently indicating liquid drops. The particles were mostly smooth throughout the penetration. At least 90% appeared to be liquid, although it could have been more because the ones classed as irregular were quite small and therefore hard to identify. This is in sharp contrast to the particles found in the main storm complex at temperatures <0°C, which had varying degrees of roughness. That nearly all the 2D-C particles appeared to be liquid is interesting because the aircraft was only a few hundred meters below the level of the -3°C penetrations of Storm A. The particles in the line were mainly drops 1 mm or less in diameter. Number concentrations were about 1 per liter and mass concentrations were <0.5 g/m^3. Weak updrafts (about 5 m/s) were present along with low values of cloud LWC. There was little sign of electrical activity during the penetration.

With only one penetration, it is difficult to draw firm conclusions about the precipitation mechanism in the line. However, with rather weak updrafts in which mm-sized drops appeared around the melting level, and cloud tops reaching only about 7 km (-16°C), it is difficult to imagine an ice process being the major factor. For example, it is difficult to see how ice particles could have melted so near the 0°C level. An independent analysis of first echoes on this day has indicated a mean first-echo temperature of +8°C, again counter to expectations for an ice process.

4. SUMMARY

The storm complex on 10 July 1989 was weak dynamically, but was characterized by a remarkable persistence in one of its storms and in a weak line that developed adjacent to it. The maximum reflectivity remained below the melting level in both features, even though Storm A had tops to over 11 km and the line only to about 7 km.

In Storm A, the weak to moderate updrafts and downdrafts allowed precipitation particles to descend and grow slowly in the small, but widespread, amounts of cloud liquid encountered. The development of maximum reflectivities below the melting level in the cloud reflects this mechanism. A wide variety of ice particles exhibiting varying degrees of riming, but mostly graupel according to images from the 2D-C probe, was found in the storm. Presumably, the larger particles were graupel or small hail. While the reflectivity maxima were at temperatures >0°C, it appears that growth of ice particles was the dominant precipitation-forming mechanism in view of the weak updrafts and the rough appearance of the hydrometeors at temperatures <-3°C.

The clouds in the line were less tall than those associated with Storm A, and particles found near the melting level were smooth and round, like raindrops. Drop concentrations were typical of light rain. The nature of the particles and the weak updrafts suggest a coalescence process, but an ice process cannot be ruled out.

Acknowledgments. Support for this research was provided by the National Science Foundation (NSF) under Cooperative Agreements ATM-8620145 and ATM-9104474; NSF Grant No. ATM-8720252; and the NOAA Federal/State Cooperative Program under agreements NA 90OAA-H-OA176, NA 17RA0218-01 and NA 27RA0178-01 through the North Dakota Atmospheric Resource Board.

REFERENCES

Boe, B. A , J. L. Stith, P. L. Smith, J. H. Hirsch, J. H. Helsdon, Jr., A. G. Detwiler, H. D. Orville, B. E. Martner, R. F. Reinking, R. J. Meitin and R. A. Brown, 1992: The North Dakota Thunderstorm Project: A cooperative study of High Plains thunderstorms. *Bull. Amer. Meteor. Soc.*, 73, 145-160.

Detwiler, A. G., J. H. Helsdon, Jr., and D. J. Musil, 1990: Evolution of a band of severe storms. Preprints, *Conf. Atmos. Elec.*, Kananaskis Provincial Park, Alberta, Canada, Amer. Meteor. Soc., 705-709.

APPENDIX F

Atmospheric Research, 28 (1992) 197–226
Elsevier Science Publishers B.V., Amsterdam

Fields of motion and transport within a sheared thunderstorm

Roger F. Reinking[a], Rebecca J. Meitín[b], Fred Kopp[c], Harold D. Orville[c] and Jeffrey L. Stith[d]

[a]*National Oceanic and Atmospheric Administration, Wave Propagation Laboratory, Boulder, CO 80303, USA*

[b]*Cooperative Institute for Research in the Environmental Sciences, University of Colorado, Boulder, CO 80303, USA*

[c]*Institute of Atmospheric Sciences, South Dakota School of Mines and Technology, Rapid City, SD 57701, USA*

[d]*Atmospheric Sciences Department, University of North Dakota, Grand Forks, ND 58202, USA*

(Received July 5, 1991; revised and accepted December 22, 1991)

ABSTRACT

Reinking, R.F., Meitín, R.J., Kopp, F., Orville, H.D. and Stith, J.L., 1992. Fields of motion and transport within a sheared thunderstorm. In: J.L. Sánchez (Editor), Agriculture and Weather Modification. Atmos. Res., 28: 197–226.

The fields of motion within a small, strongly sheared High Plains thunderstorm are examined using measurements of reflectivity and velocity from an airborne Doppler radar and other in situ measurements. The measurements are complemented by a high resolution two-dimensional numerical simulation of the storm. Implications for predicting storm characteristics, delivery and effectiveness of seeding material, and precipitation efficiency are examined. The numerical model run was made in the forecasting mode 5 h before initial storm development and 7 h before the observations of the mature stage. The main features of the simulated storm structure and motions are very similar to those measured, except that the model produced a vertically and temporally compressed storm. The characteristics of the measured and the modeled storm, in combination, are consistent with other theories and observations that precipitation efficiency is low and a large portion of the processed water substance is transported out through the anvil in thunderstorms that develop in an environment with strong wind speed shears in the vertical. The measurements and the model reveal a quasi-steady-state organization during the mature stage. Although the storm formed in response to surface heating, the simulation and the radar measurements in combination indicate that the relative importance of inflow directly from the surface was diminished during the mature stage and completely cut off during the dissipation stage. Despite the modest size and intensity of this storm, the actual circulation within it was highly three dimensional and this, of course, could not be directly simulated by the two-dimensional model. Mature-stage inflows between about 3 and 6 km above ground level from a south-flank feeder cell field contributed significantly to the main updraft. Effective delivery of cloud seeding material to a storm like this would be influenced by the three-dimensionality and the relative importance

Correspondence to: R.F. Reinking, National Oceanic and Atmospheric Administration, Wave Propagation Laboratory, Boulder, Colorado 80303, USA.

of surface feeding in relation to inflows from levels above the surface. Such features would have to be determined in real time and state-of-the-art technologies offer the means to do this.

RÉSUMÉ

Les champs de vent a l'intérieur d'un orage des "High Plains", de petite taille et caractérisé par un important cisaillement, sont examinés au moyen de mesures de la réflectivité et de la vitesse du vent enregistrées à partir d'un radar Doppler aéroporté et d'autres mesures in situ. L'utilisation d'un modèle de simulation à 2 dimensions du développement de nuages convectifs complète l'étude. Les implications pour la prévision des caractéristiques des orages, ainsi que le degré d'efficacité du matériel d'ensemencement et son importance sur les précipitations sont discutées.

Le modèle numérique de prévision a été initialisé pour 5 heures précédant le début de l'orage et 7 heures avant son étape de maturite. Les caractéristiques principales de la structure de l'orage et de ses mouvements sont très proches de celles mesurées, à la différence près que le modèle en produit une image verticale et temporelle comprimée. Les mesures et le modèle confirment d'autres théories et observations sur les orages qui prétendent que, en présence d'un environnement à fort cisaillement vertical, la part de précipitation est faible et qu'une grande quantité de l'eau condensée est transportée à travers l'enclume.

Malgré la taille et l'intensité modestes de cet orage, la circulation interne des courants était fortement tridimensionnelle, ce qui, évidemment, ne pouvait être directement simulé par le modèle à 2 dimensions. Les mesures et le modèle ont mis en évidence une organisation quasi stationnaire pendant la période de maturite.

Bien que l'orage se soit développé en réponse à un réchauffement de surface, le modèle et les mesures in situ indiquent une diminution de son importance relative lors de la période de maturité et un découplage lors de la phase de dissipation. Ce sont les courants générés par des cellules du flanc sud, localisées entre 3 et 5 km au-dessus du sol qui fournissent une alimentation substantielle au mouvement vertical principal. Le transport effectif du matériel d'ensemencement pour un orage de ce type semble être influencé par des paramètres tridimensionnels ainsi que par l'importance relative de l'alimentation de surface par rapport à celle des couches plus elevées. L'utilisation de techniques de pointe devrait permettre l'étude en temps réel de telles caractéristiques.

APPENDIX G

A North Dakota First-echo Analysis

by

John W. Stoppkotte

A thesis submitted to the Graduate Division

In partial fulfillment of the requirements

for the degree of

MASTER OF SCIENCE IN METEOROLOGY

SOUTH DAKOTA SCHOOL OF MINES AND TECHNOLOGY

RAPID CITY, SOUTH DAKOTA

1993

Prepared by :

John W. Stoppkotte

Approved by :

Paul L. Smith

Major Professor

Harold D Orville

Chairman, Department of Meteorology

May 18/1993

Dean Graduate Division

A North Dakota First-echo Analysis

John W Stoppkotte
Institute of Atmospheric Sciences
South Dakota School of Mines and Technology

ABSTRACT

Radar data from North Dakota field projects conducted in the summers of 1987 and 1989 were studied by means of first-echo analysis to shed light on the underlying microphysical processes. For the two years combined, the average first-echo height (FEH) was calculated to be 4.83 km above mean sea-level (MSL) with an average first-echo temperature (FET) of -4.3 °C. The comparison of first-echo parameters to cloud base temperatures and to in-cloud transport times determined from a one-dimensional steady-state cloud model showed little or no value in the prediction of first-echo characteristics. The correlation between FEH and the height of the 0 °C level was stronger, suggesting the importance of temperature (and, by implication, ice process) in first-echo development. The relationship of maximum updraft speed to certain first-echo parameters also exhibited a somewhat better correlation, but not to the extent that the updraft alone could be used as a predictor of first-echo characteristics.

The majority of first-echo temperatures were lower than 0 °C, except for 28 June 1987 and 10 July 1989, in which the average first-echo temperature for the day was +1.9 °C and +8.3 °C respectively. These case days were studied more carefully in reference to synoptic conditions and upper-air analysis in the belief that the type of air mass may affect first-echo height and, therefore, temperature. Both days included parcels with predicted updraft speeds of near 10 m/s or less. This first-echo data suggests that warm rain processes may also be of importance in some North Dakota convective clouds.

Also included in this study is an investigation of reflectivity thresholds from which to study first-echo occurrences. Some reflectivity threshold must be used in order to determine the point at which the radar will be detecting actual precipitation. Although an exact value of the onset of actual precipitation cannot be defined, an effective "gray area" between detection of clouds and detection of precipitation can be located.

Reprinted from the preprint volume of the 26th International Conference on Radar Meteorology, 24-28 May 1993, Norman, OK. Published by the American Meteorological Society, Boston, MA.

19.3

APPENDIX H

WHAT IS A "FIRST ECHO"?

John W. Stoppkotte and Paul L. Smith

Institute of Atmospheric Sciences
South Dakota School of Mines and Technology
501 E. St. Joseph Street
Rapid City, South Dakota 57701-3995

1. INTRODUCTION

Early development of radar echoes in small cumulus clouds has become a subject of renewed interest. Charles Knight and colleagues have used high-sensitivity radars in the North Dakota Thunderstorm Project (NDTP) and the Convection and Precipitation/Electrification (CaPE) project to demonstrate how echo intensities evolve from essentially "clear-air" reflectivity values to ones that are characteristic of precipitation (Knight and Miller, 1990; Knight *et al.*, 1992). The increasing echo intensities that accompany cloud and precipitation formation are a continuous process, which brings into question the use of a fixed "first-echo" threshold as an indicator of precipitation initiation. Previous studies of first-echo characteristics have used a fixed reflectivity threshold, or sometimes just a minimum detectable echo, as an indicator of when and where precipitation is beginning. Our purpose here is to reexamine that issue from a microphysical perspective.

An important step in precipitation initiation is the critical period when hydrometeors first grow large enough that further growth by collection of cloud droplets happens quickly. The accompanying rapid increases in particle size may lead to increases in reflectivity that are identifiable by radar. Once some water drops get large enough to grow rapidly by coalescence (or ice crystals by accretion), the beginning steps to further precipitation in the cloud are obscured to radar because of the strong influence of the largest particles on reflectivity values. For first-echo analysis to have meaning in terms of precipitation initiation, it is necessary to find some threshold of reflectivity to which early hydrometeor growth can be related.

Any combination of hydrometeor sizes and number concentrations carries with it associated values of liquid water concentration, rainfall rate, and reflectivity factor. Examination of the relationships among them may shed some light on the possibility of establishing a meaningful first-echo threshold. An upper boundary on these values for precipitation-free clouds can be established by considering various known characteristics of such clouds. A more difficult question is whether a corresponding lower bound can be established on the reflectivity values associated with precipitation and whether such boundary will overlap clear-air-type reflectivities or those of clouds containing no precipitation significantly. The "gray area" between the two boundaries, where the echo might be due to either cloud or precipitation, could serve as an indicator of the confidence with which one can identify the onset of precipitation on the basis of reflectivity values alone.

2. PROCEDURE

The analysis here examines various factors that affect the width of the "gray area" in an effort to identify considerations which might lead to meaningful specification of a first-echo threshold. For purposes of illustration we assume a monodisperse distribution of water droplets and represent the various quantities of interest on a composite diagram (Fig. 1). Actual droplet distributions are not monodisperse, but many have a pronounced modal character and use of the number concentration along with a size measure such as an appropriately-weighted mean diameter will make the diagram at least roughly applicable in practical situations.

The basic equations involved are for reflectivity factor:

$$Z = N_t D^6 \quad ,$$

liquid water concentration (LWC):

$$W = (\pi\rho/6)\, N_t D^3 \quad ,$$

and rainfall rate:

$$R = (\pi/6)\, N_t D^3 V_t \quad .$$

Here N_t represents the number concentration, D the drop diameter, and V_t the corresponding terminal fall speed.

Various combinations of droplet diameter and concentration were used in a spreadsheet environment to calculate associated values of

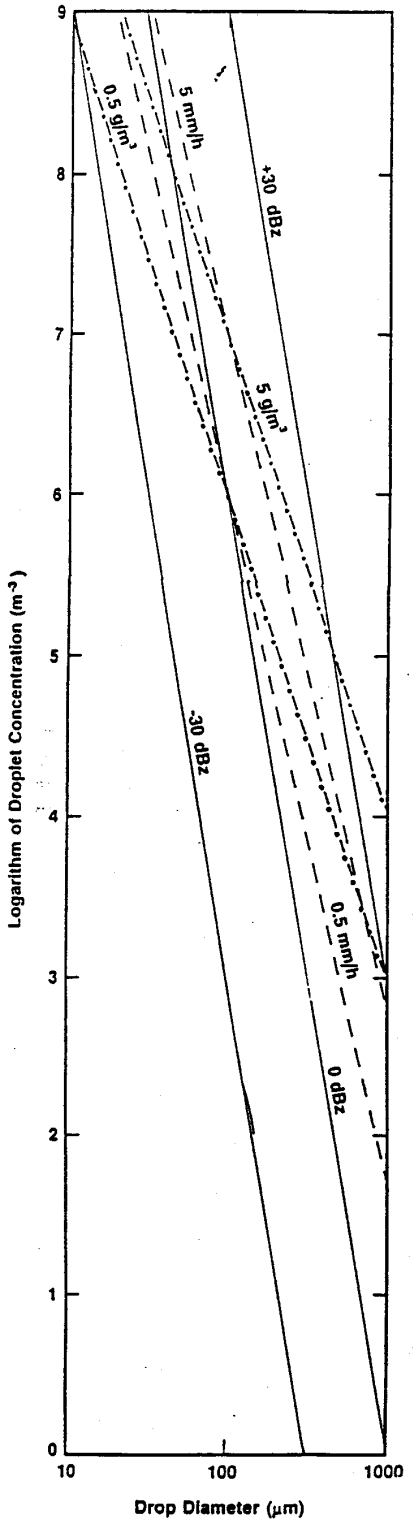

reflectivity, LWC, and rainfall rate. Reflectivity isolines of -30, 0, and +30 dBz are plotted in the figure along with ones for LWC of 0.5 and 5 g/m^3 as well as rainfall rates of 0.5 and 5 mm/h. These values were chosen because of their relationship to the development of precipitation.

3. RESULTS

The first thing apparent from Fig. 1 is that particle size is, in general, more important than number concentration in determining the reflectivity factors. For example, the appearance of raindrops several tenths of a millimeter in diameter, even in fairly low concentrations, would push Z above the range of plausible values for clouds. Moving from upper left to lower right across the diagram, in the direction of increasing particle size, an upper limit on the reflectivity (for "non-precipitating" cloud conditions) is set first by the plausible limits on the LWC, then by the rainfall rate, and finally by the drop sizes themselves. The figure indicates that above an upper reflectivity boundary near 10-15 dBz one could assume, with reasonable confidence, that precipitation is occurring.

At the other extreme, the figure reveals (for example) that at concentrations of 10^6 m^{-3} (or 1 cm^{-3}) a 0 dBz value could indicate the onset of precipitation as well. Yet Knight and Miller (1990) discuss findings of very early cloud echoes in the neighborhood of -25 to -10 dBz, even as high as -5 dBz; this seems to be quite reasonable when looking at Fig. 1 in terms of droplet sizes and concentrations corresponding to those found in clouds. Thus the demarcation between cloud echoes and precipitation echoes in this range of reflectivities is not clear-cut. However, the growth of particles large enough to produce reflectivities of 0 dBz tends to be quite rapid, so the accompanying evolution of Z may reduce the need for concern about an exact threshold (Fig. 2).

The dual-wavelength work in Knight *et al.* (1992) indicates that the earliest echoes come from refractive-index variations, usually from turbulent mixing of air with different values of humidity and temperature associated with the cloud development. There is nearly always a radar echo at about -20 dBz from the very onset of visible condensation due to this Bragg scattering, not Rayleigh backscattering from the hydrometeors. This finding as well as information inferred from Fig. 1 emphasizes the fact that reflectivity factors below this level would not be of concern for first-echo studies.

Fig. 1: Diagram relating reflectivity factors to liquid water concentrations and rainfall rates for various monodisperse drop size distributions. Solid isolines represent reflectivities; dash-dot lines are LWC's; and dashed lines are rainfall rates.

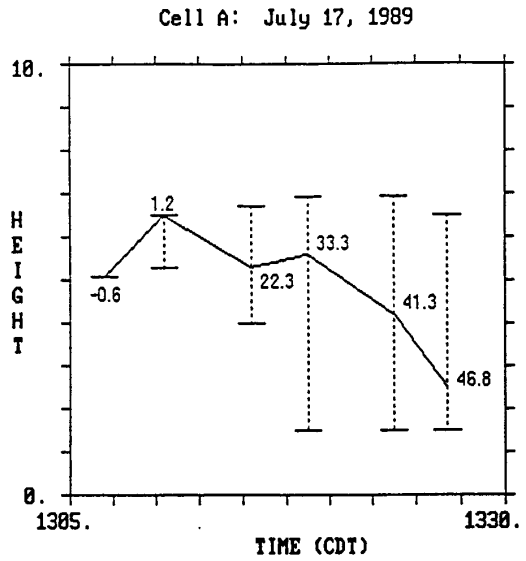

Fig. 2: History of NDTP Cell A on July 17, 1989. Numbers in the graph represent the maximum reflectivity factor at each scan time (dBz). Solid line indicates height (km) of maximum reflectivity factor. Dashed lines represent vertical limits of -5 dBz echo.

The dual-wavelength observations clearly show the development of Rayleigh-scattering echoes from the growing hydrometeors, but the degree to which they imply precipitation development remains to be clarified. This analysis identifies the "gray area" problem as lying primarily in the establishment of a suitable lower reflectivity boundary when considering the distinction between cloud reflectivity values and those of precipitation.

4. DISCUSSION

Previous first-echo studies have typically used a threshold such as 15 or 20 dBz (and sometimes not clearly defined) to identify areas of presumed initial precipitation and, hence, to determine first-echo hights. The high-sensitivity observations by Knight and Miller (1990) and Knight *et al.* (1992) have cast some doubt upon the relation of first-echo height to precipitation development processes because of the ill-defined transition from cloud to precipitation echoes. The widespread appearance of 0 dBz echoes before the initial appearance of 20 dBz in a vigorous cumulus cloud is a reflection of this. The present analysis is designed to elucidate that gap and shed some light on how to interpret and evaluate first-echo data. If the reflectivity increases in a fairly confined altitude band from, say, 0 dBz to 20 dBz in a few minutes, the difference between 5 or 10 or 15 dBz as a first-echo threshold may be immaterial for many purposes.

It is well understood that the threshold value chosen for first-echo studies can significantly affect first-echo-height determinations and, ultimately, the inferences regarding various precipitation processes. Studies such as those by Knight and colleagues using high-sensitivity and dual-wavelength radar data can aid in answering the ongoing question of the value of first-echo observations in the determination of precipitation initiation. Supporting aircraft observations to establish the microphysical and kinematic characteristics of the clouds in transition to the precipitating stage would be a valuable complement to such studies. The generality of the rapid increases in echo intensity across the 0 - 20 dBz interval should also be determined.

Although some doubt exists about the relationships between first-echo height and precipitation processes, this threshold analysis could indicate new directions from which to tackle this problem. The renewed interest in small cumulus clouds and the need to identify precipitation processes key the need for further analysis and further studies to try to understand the problem and narrow the width of the reflectivity "gray area".

Acknowledgments. This research was sponsored by NOAA-North Dakota Cooperative Agreement NA17RA0218-01 under contract ARB-IAS-91-02 with the North Dakota Atmospheric Resource Board and NOAA-North Dakota Cooperative Agreement NA27RA0178-01 under contract ARB-IAS-92-01.

REFERENCES

Knight, C. A., and L. J. Miller, 1990: First 5-cm radar echoes at low dBz values in convective clouds. Preprints, *1990 Conf. Cloud Physics,* Amer. Meteor. Soc., San Francisco, CA, 716-721.

Knight, C. A., L. J. Miller and N. C. Knight, 1992: Dual-wavelength study of early cumulus in Florida. Preprints, *11th Int'l. Conf. on Clouds and Precip.,* Montreal, 429-432.

APPENDIX I

Summary of Continuing First-Echo Studies from the 1989 North Dakota Thunderstorm Project

by

Daran L. Rife

I. Introduction

This is a continuation of the first-echo studies performed by Stoppkotte and Smith (1993) and Knight and Miller (1993). The focus of this facet of the first-echo study was to attempt to determine a meaningful first-echo reflectivity threshold, and learn how this threshold affects the height of the first echo as seen by radar. We also sought to answer the question of how range of the first echo from the radar affects first-echo height, and whether first-echo studies are meaningful at substantial distances from the radar. Finally, we were interested in determining if there is any effect on first-echo height due to differences in local synoptic conditions.

II. Analysis Method

Stoppkotte had listed possible radar first echoes from the North Dakota Thunderstorm Project for each day studied on computer disk. This listing contained the time of the radar scan in which each first echo was located; the azimuthal, range, and height location of the first echo; and its reflectivity value. The radar scan data are stored digitally by date and time on computer tapes. If one wishes to analyze a particular day's data, the tape containing the desired data must be loaded into the Interactive Radar Analysis System (IRAS, Priegnitz and Hjemlfelt, 1993). Using the display and interrogation capabilities of IRAS, the user can then locate and identify radar echo features within the radar scan quite readily.

The intention of this study was to locate each of the first echoes identified by Stoppkotte in the stored radar scan data, and follow its development from 0 - 20 dBz in reflectivity. This development information was used to create "life histories" of these echoes. The information contained in the life histories included: scan time (CDT), azimuthal position of first echo in the radar scan, range from the radar to the maximum reflectivity region, elevation angle of the radar, height of the maximum reflectivity within the first echo, first echo top and base (> -20 dBz), and the value of the maximum reflectivity within the first echo. The information from each first-echo life history was subdivided into reflectivity threshold categories, with values of <5, <10, <15, <20, and >20 dBz. This information was then used to plot first-echo heights as a function of reflectivity threshold, on a time-base scale.

Plots to illustrate the effect of reflectivity threshold on the indicated first-echo height, relative to that found using a 10-dBz reference threshold, were created for each first echo. The echo histories were also divided into three groups of roughly equal size by

increasing range, and composite plots were made to search for range-dependent effects. The three range categories are ≤ 80 km, 80 - 100 km, and 100 - 140 km.

III. Results and Discussion

Problems were found with some of the entities that Stoppkotte identified as first echoes. He had used a version of IRAS that ran on a low-resolution PC. When re-identifying these first echoes using the X-WINDOWS version of IRAS on a very high resolution workstation, it was evident that many of the first echoes identified using the PC system were actually clutter, aircraft, chaff, underneath existing storm anvils, or connected to existing storms. Much of the data provided by Stoppkotte had to be eliminated for one of the aforementioned reasons. It then became necessary to search the entire store of radar scan data for each day to locate "good" first echoes. Thirty-one such echoes were identified and their life histories collected.

Figure I-1 shows example plots of the height of the maximum reflectivity for the first echoes that grew to 20 dBz in reflectivity (many died out shortly after reaching 20 dBz; most did not grow to any appreciable height). Notice that there are few examples of nearly constant "first-echo" height, and also no apparent uniform pattern of change, e.g., increase (decrease) in first-echo height, as the reflectivity threshold (indicated by the shading) increases. The evolution patterns of most of the echoes are unpredictable.

Figure I-2 shows the effect of reflectivity threshold on the change in first-echo height relative to that found with a 10-dBz reference threshold, for different range intervals. The maximum width of the beam for each range category is drawn on the plots as well, to give an idea of the height resolution capability of the radar. The object was again to identify any systematic trend in the height of the first echoes dependent on the reflectivity threshold. In the ideal case, absence of any significant variation as the threshold increased would suggest that the first-echo height should be a good indication of the level of initial development of precipitation. Any systematic height variation could possibly be related to growth of the precipitation particles in updraft (downdraft) regions. From the standpoint of "classical" first-echo analysis, one would expect (or at least hope for) the absence of any trend. Referring to Fig. 6 as well as Fig. I-2, there is certainly a variation of first-echo height with the threshold, that is greater than the beamwidth resolution capability at the shorter ranges. Moreover, there is no consistent height trend for the first echoes as they pass each successive reflectivity threshold. First-echo height tends to vary in an irregular manner with the threshold, so that there is no clearly-defined height for the initial appearance of precipitation.

At ranges beyond 80 km in Fig. I-2, it makes little difference what reflectivity threshold is used because the differences in first-echo height are less than the radar beamwidth in most instances. This is probably a consequence of the limited vertical resolution in the data, rather than any homogeneity in the first-echo heights. The width of the beam at ranges greater than 80 km does not allow the resolution required to see differences in echo height less than about 1.5 km. This suggests that if first echoes are to be studied, then the echoes should be close to the radar; a range closer than 60 km would

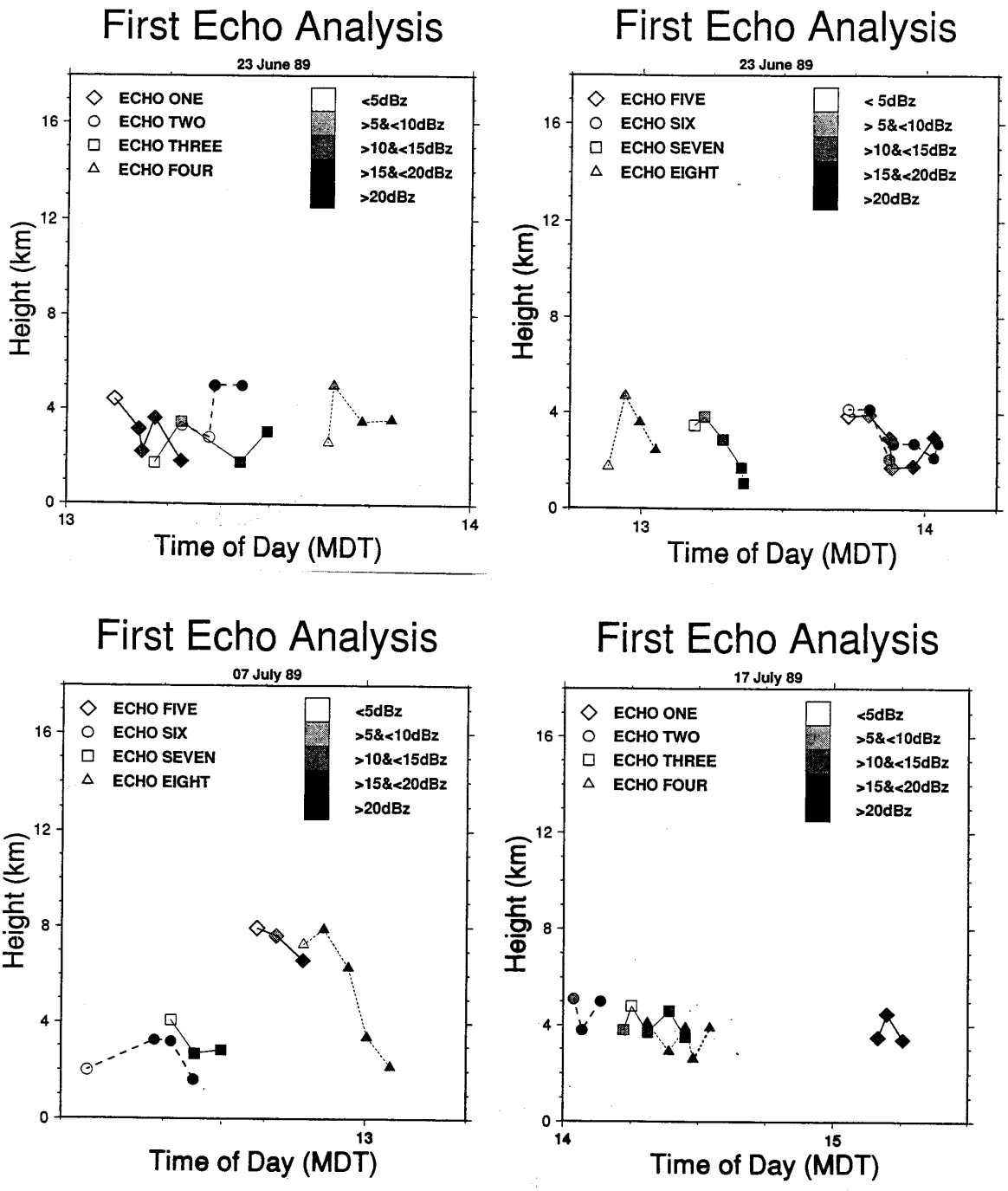

Fig. I-1: Plots of the height of maximum reflectivity with time, for the "first echoes" that grew to about 20 dBz and died out shortly thereafter. The plots are divided by day. Shading of symbols indicates which reflectivity threshold has been exceeded at the time of the scan.

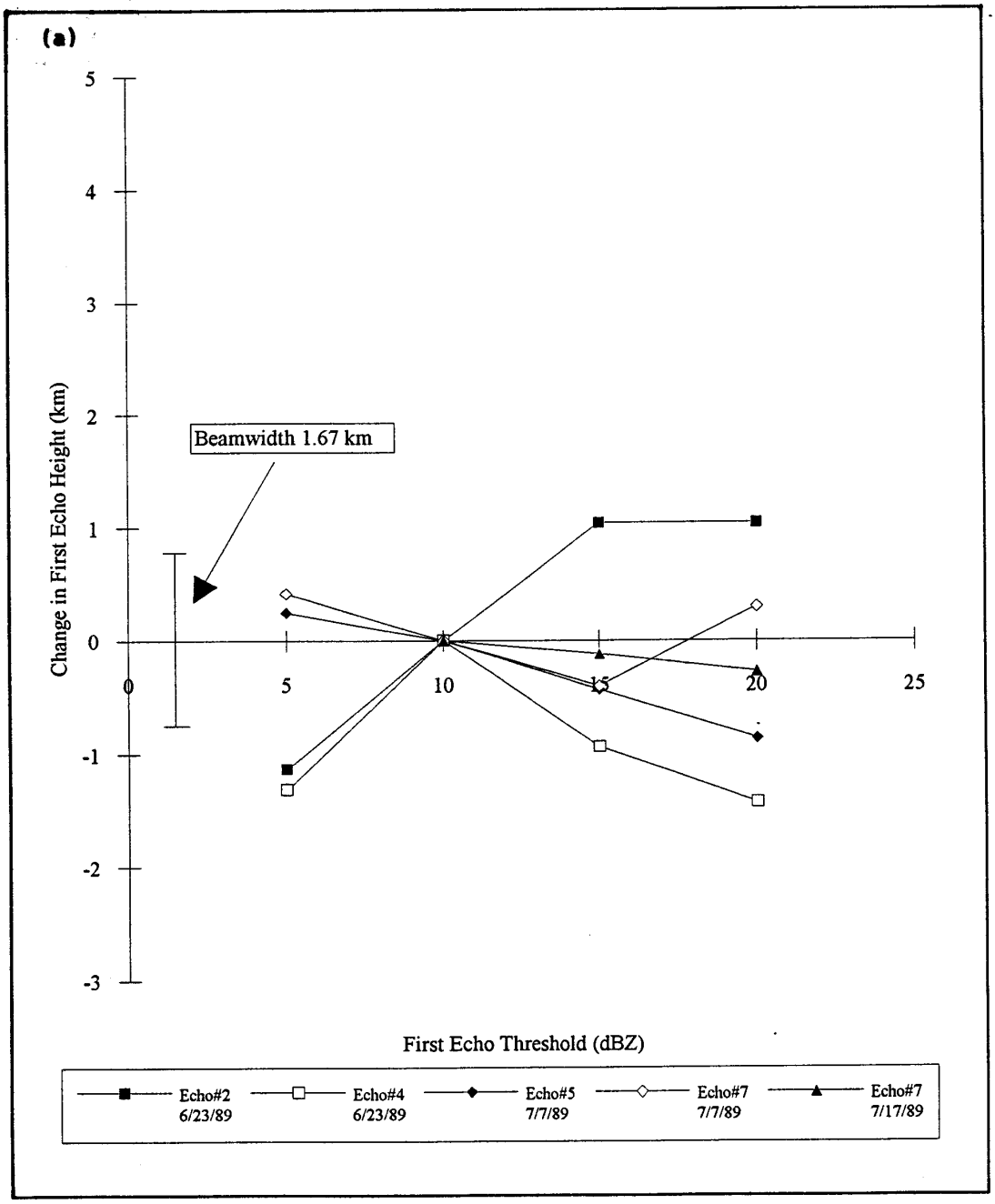

Fig. I-2: The effect of reflectivity threshold on the first-echo height, plotted relative to that found with a 10-dBz reference threshold. These composite plots were created by dividing the first echoes into three groups of roughly equal size, by increasing range.

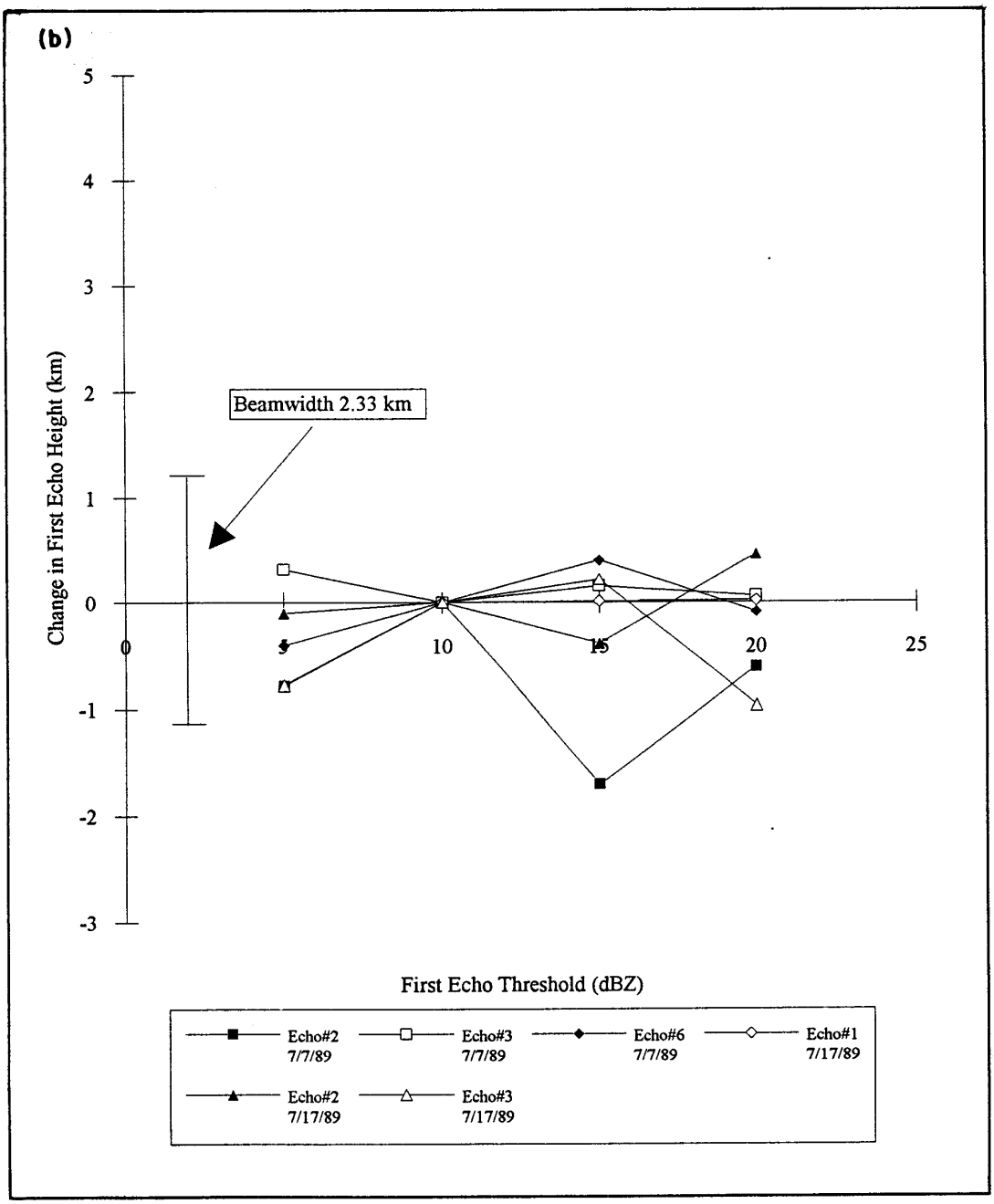

Fig. I-2: (cont'd.) Approximate radar beamwidths are shown to indicate the limitations of the vertical resolution of the radar. (a) For 80 < r < 100 km; (b) for 100 < r < 140 km. (The corresponding plot for r < 80 km appears in Fig. 6 of the main body of this report.)

be preferable. At ranges less than 60 km, the radar beam will be less than 1 km wide (for a one degree beamwidth); this will improve our ability to "see" the early evolution of cloud microphysical processes.

An interesting finding is that more than 95% of the first echoes analyzed had very short lifetimes; most were visible (on radar) for slightly less than 15 minutes. Although our sample is quite small, our data can be compared to the findings of Johnson and Dungey (1978), who used data from projects where the radar was specifically set up to detect and track first echoes. They sampled 2260 first echoes from two days of the Whitetop Project and found that more than 50% of the echoes sampled had lifetimes of 15 minutes or less. They found, as we did, that 95% of the clouds producing first echoes are rather small entities and do not grow into larger convective clouds, nor do they merge with any other clouds. Most first echoes are so small that they are mixed out or rain out shortly after reaching 20 dBz in reflectivity.

These observations led us to concentrate on those first echoes that later grew beyond 25-dBz reflectivity. This action should eliminate from consideration any first echo that did not result in precipitation at the surface during its lifetime. The radar scan data were then analyzed again (for each of the days stored) to find first echoes that grew beyond 25 dBz. Figure I-3 shows the effect of reflectivity threshold on first-echo height, relative to a 10-dBz reference, for a sample of first echoes that grew beyond 25 dBz in reflectivity. As in Fig. I-2, Fig. I-3 again shows that first-echo height tends to vary with the threshold, so that there is no clearly-defined height for the initial appearance of precipitation.

Figure I-4 also shows the change in first-echo height relative to a 10-dBz reference, but here the plots are grouped by day. The object here was to identify any regular variation in first-echo heights that might be due to differences in synoptic conditions. The figure and similar ones for other days show that no clearly-defined height variation of first echoes due to differences in synoptic conditions can be identified.

IV. Conclusions and Recommendations

It is difficult to determine the initiation of precipitation from observations of first echoes, with reflectivities less than 20 dBz. First-echo height tends to vary in an irregular way with the reflectivity threshold used, which makes it difficult to determine the level of initiation of precipitation. It would be preferable to use ranges less than 60 km to study the precipitation processes by first echoes using weather radar, and also to concentrate on only those echoes that eventually achieve reflectivities greater than 25 dBz. At ranges beyond 80 km, the radar does not allow the vertical resolution necessary to ascertain differences in first-echo height. The latter action would tend to eliminate from consideration any first echoes that did not result in precipitation at the surface during their lifetime; 95% of the first echoes we studied never grew to this storm stage. Even so, it is not clear how closely the first-echo observations can be related to the initiation of precipitation.

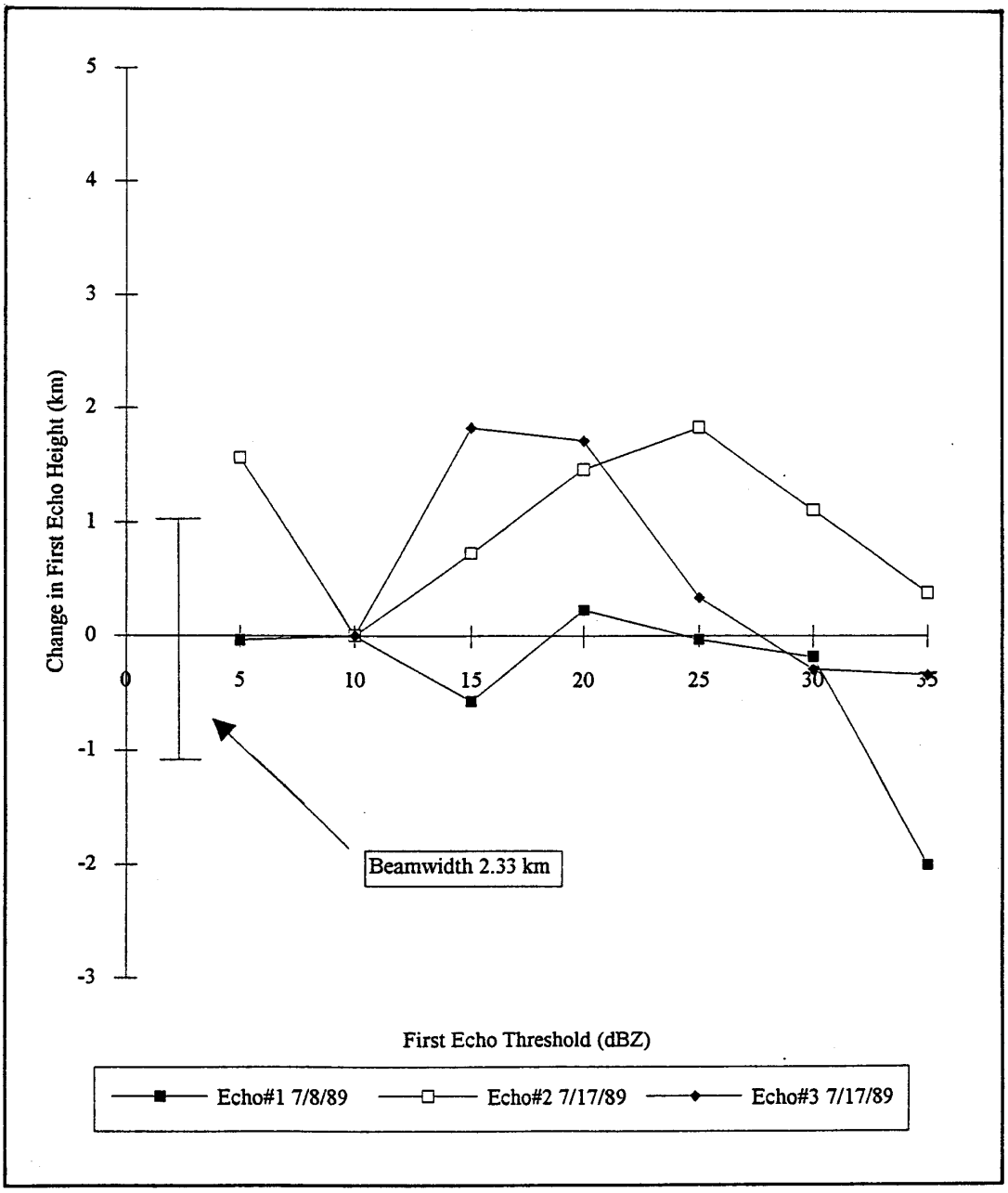

Fig. I-3: Similar to Fig. I-2, but for echoes that grew beyond 25 dBz in reflectivity.

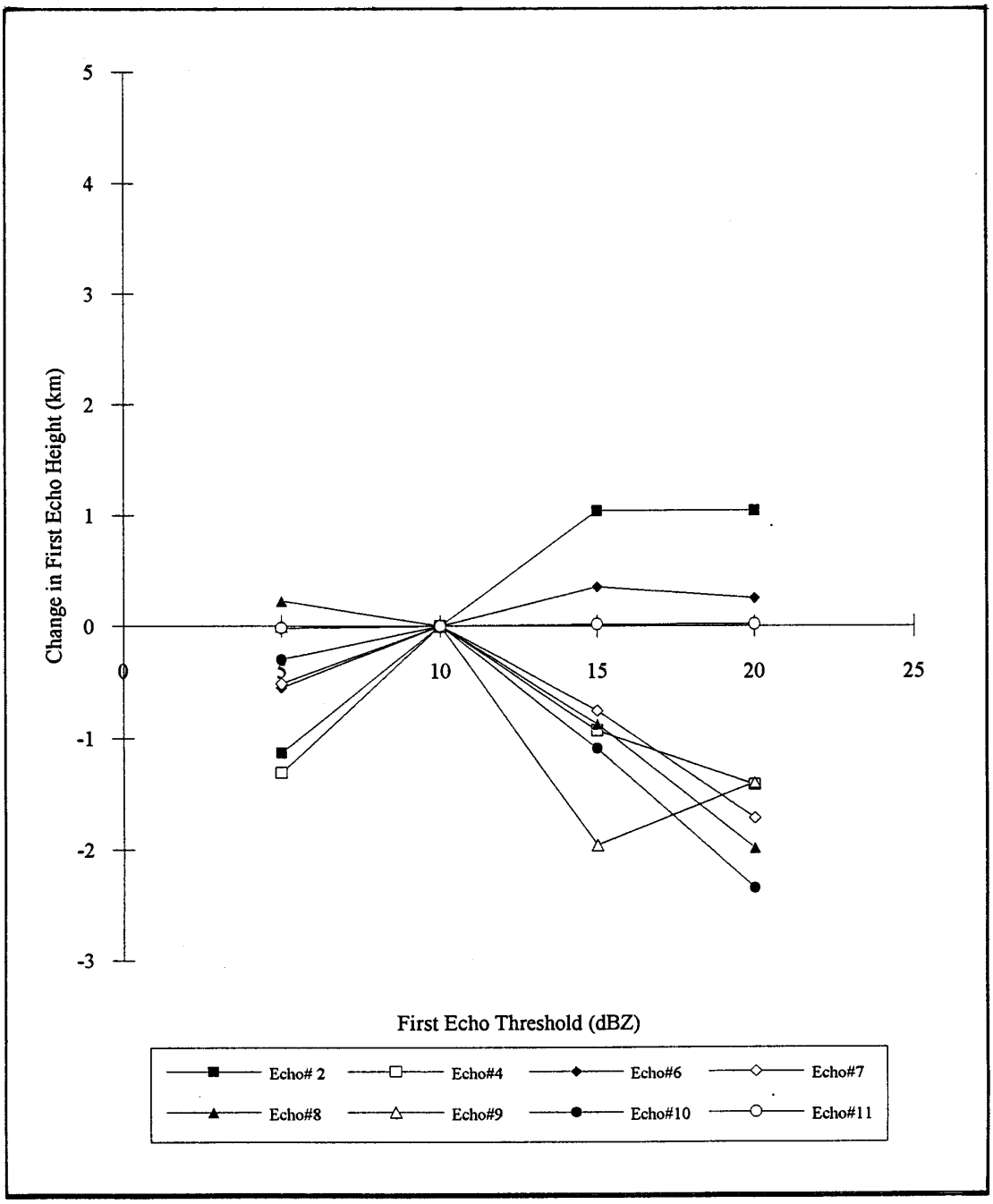

Fig. I-4: Similar to Fig. I-2, but for a group of echoes from the same day (23 June 1989).

Reprinted from the preprint volume of the **26th International Conference on Radar Meteorology**, 24-28 May 1993, Norman, OK. Published by the American Meteorological Society, Boston, MA.

11.4

APPENDIX J

SUN-IRAS: AN IMPROVED PACKAGE FOR THE DISPLAY AND ANALYSIS OF WEATHER RADAR DATA

David L. Priegnitz and Mark R. Hjelmfelt

Institute of Atmospheric Sciences
South Dakota School of Mines and Technology
501 E. St. Joseph Street
Rapid City, SD 57701-3995

1. INTRODUCTION

One of the main benefits from the rapid advances in today's computer technology has been the affordability of high-resolution Unix-based workstations. Most of these workstations are capable of processing and displaying large amounts of information in multiple windows, something affordable to only a limited group only a few years ago.

One type of information which is ideally suited for analysis and display on these workstations is digital weather radar data. Several software packages exist for this purpose. One of the oldest, the NCAR Interactive Doppler Editing Software (IDES) (Oye and Carbone, 1981), has been ported to a number of hosts. Its main strength is in editing Doppler velocities for windfield reconstruction. More recently, the NCAR *zeb* software package (Corbet and Mueller, 1991) provides a graphical user interface to select and display radar and other types of meteorological data. It has been designed to operate in real-time and post-analysis modes. Its strength is in its ability to display many different types of meteorological information in addition to Doppler radar data. Priegnitz, (1991) developed the Interactive Radar Analysis Software (IRAS) package specifically for the display and analysis of weather radar data on a personal computer running under MS-DOS. Its main strength is in its ability to perform detailed analysis of single (Doppler) radar data on a low-cost personal computer.

Recently, IRAS has been migrated to the Sun SPARCstation. Its main advantages over its predecessor are the improved user interface and the ability to add new functions easily. This paper describes the features available with this version of IRAS (hereafter referred to as Sun-IRAS) including comparisons with the PC version (hereafter referred to as PC-IRAS).

2. PC-IRAS VS. SUN-IRAS

Although PC-IRAS provides the radar analyst with a number of useful functions to help in the analysis of weather radar data, a number of limitations are imposed by the hardware and software. Depending on the type of processor used (80286, 80386, or 80486) or whether or not a math coprocessor is available, PC-IRAS data processing can either be slow or very fast. The display software is designed for EGA mode, so screen resolution is limited to 640x480 pixels and 12 colors for data. In addition, the program size limitation imposed by the MS-DOS operating system makes it a problem to add new functions. Depending on the amount of free memory, PC-IRAS may or may not load (requires about 450 Kb). This makes trying to install PC-IRAS on different PCs very tedious since each one may have a different configuration.

Sun-IRAS provides a superior alternative to PC-IRAS. It runs on a Sun SPARCstation supporting the OpenLook Graphical User Interface and running under Unix. A friendlier interface is provided to the user. Most menus can be "pinned" for easier access. Display window size can be interactively increased/decreased by the user. Two independent Sun-IRAS sessions can be run concurrently. Each Sun-IRAS session provides 64 colors out of a palette of 16 million for radar data display. New functions can be added without having to worry about program size constraints. All code has been converted from FORTRAN to C.

3. SUN-IRAS FEATURES

Many of the features available with Sun-IRAS are presented in Table 1.

TABLE 1.

Major Sun-IRAS Features

1. Select display type from
   a. Slant PPI
   b. CAPPI
   c. Reconstructed RHI
   d. Vertical Cross Section
2. Full control of
   a. Beamwidths
   b. Display sectors
   c. Magnification
   d. Range of displayed data
3. Contouring
4. Echo Area Analysis
5. Echo Histogramming
6. Direct pixel interrogation
7. Display Labelling
8. Overlay
   a. Aircraft Flight Tracks
   b. Lightning discharge locations
   c. Maps, etc.
9. Display color thresholding
10. Color Table Editing
11. Animation

Sun-IRAS provides four main display types: PPI, CAPPI, reconstructed RHI, and vertical cross section. The later two require a PPI or CAPPI to be generated first. The size of the display window for each type can be interactively increased/decreased. Direct pixel interrogation is supported for all types except the vertical cross section. Interrogation provides information such as pixel location, value, height (MSL), and sample time. The radar beamwidth can be artificially increased/decreased for display and analysis purposes. Display center can be set for PPI and CAPPI displays along with a magnification factor. The range of data displayed can be set at any time.

A sample PPI display is presented in Figure 1.

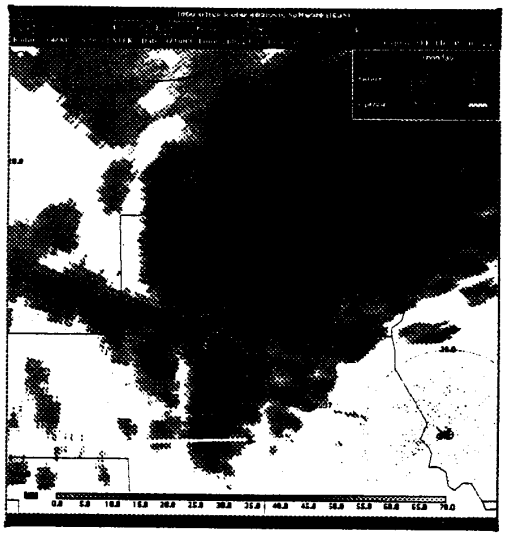

Fig. 1: Sample PPI display. Shading indicates reflectivity factors (dBz), with scale indicated along the bottom.

As also with a CAPPI display, a row of menu buttons are displayed along the top of the window. They are: **file, control, display, utilities, color, animation, clear**. Each selection may or may not generate a submenu.

File activates a menu containing a list of data filenames. This list is generated each time the file button is selected. An environment variable is used to set a default path prior to invoking Sun-IRAS. The user can select a radar data file from one of the submenus. If an invalid data file is selected, the user is provided with both an audio and visual message.

Control provides a menu of selections to control various display attributes, such as beamwidth, display sector, displayed data range, magnification, and display center. The display center can be either an offset from the radar coordinate or an actual earth coordinate specified by the user.

Display provides a menu from which the user can select an elevation angle for a PPI display or a height for a CAPPI display. A new elevation angle submenu is created whenever a new radar data file is selected.

Utilities provides a menu of the main Sun-IRAS analysis functions. Functions provided for the analysis of PPI/CAPPI displays include: contour, echo analysis, histogram, label, overlay, RHI, threshold, and vertical cross section. Each will be briefly described in the following text.

The contouring function draws contour isolines within the PPI and CAPPI display windows. The user can set the range of values contoured, the contour interval, contour line style, contour label characteristics, and smoothness of contours. A sample contoured PPI display is presented in Figure 2.

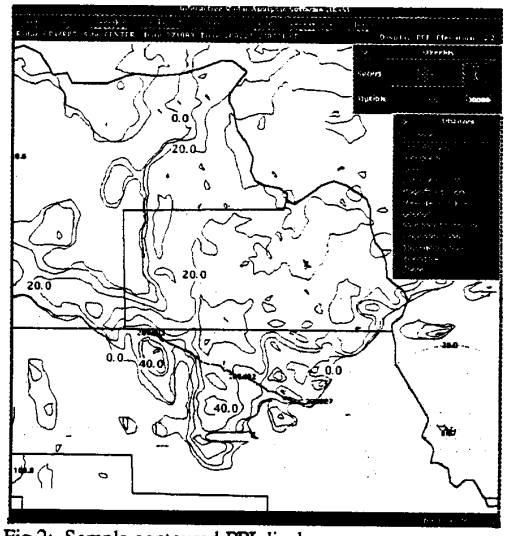

Fig 2: Sample contoured PPI display.

Sun-IRAS, unlike PC-IRAS, provides an echo analysis function which allows the user to determine various properties about an echo region. These properties include: echo area above a user-defined threshold, maximum and mean reflectivities, and maximum and mean rain rates. A sample echo analysis display is presented in Figure 3.

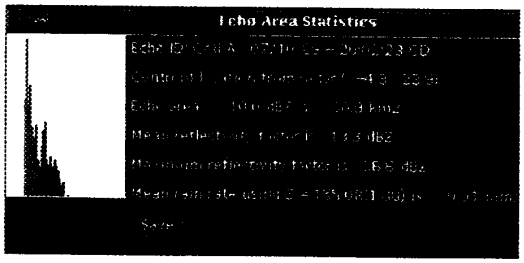

Fig. 3: Sample area analysis output.

The user has full control over the Z-R relation used to compute the rain rates. In addition, a histogram is presented showing the distibution of reflectivity values inside the echo area.

A new feature with Sun-IRAS is the ability to

interactively label any display. The user has full control of the font characteristics as well as the location of the label.

Sun-IRAS provides all of the overlay capabilities of PC-IRAS (polar and rectangular grid lines, flight tracks, and lightning locations) along with: *latitude/longitude lines, storm-relative flight tracks*, and *maps*. The user now has full control over the line style and font characteristics for the labels. In addition, it is possible to overlay other types of information, such as NWS surface synoptic station locations, project specific intrumentation locations, etc. A simple ASCII format is used so that new overlays can be generated with a text editor.

As mentioned earlier, Sun-IRAS provides a function for reconstructing RHIs from a radar volume. The user defines the radial for the reconstructed RHI by picking a point on a PPI or CAPPI display. A sample RHI display is presented in Figure 4. RHI displays can be generated with the vertical and horizontal scales the same or different.. A subset of utility functions is available for RHI displays. These include: grid overlays, contouring, and labelling. In addition, a function is provided for manual identification of first-echo information. This information can be stored to a file for later analysis.

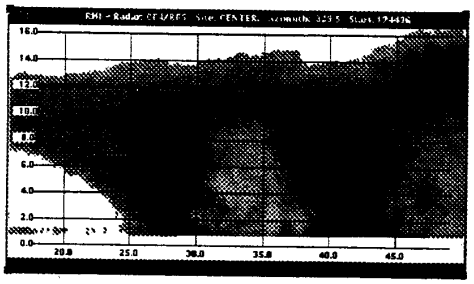

Fig 4: Sample RHI display with identical vertical and horizontal scales (in kilometers).

A color thresholding function is provided to allow the user to selectively turn on or off a range of displayed values. This is especially useful for locating echo cores to determine echo movement.

The vertical cross section function. as with the reconstructed RHI function, generates a display after a PPI or CAPPI is displayed. The user defines the horizontal end points by selecting two points on a PPI or CAPPI display, and a vertical section along the line joining those points is generated. A sample vertical cross section is presented in Figure 5. As with the RHI display, the same subset of functions is available for vertical cross section displays.

Color invokes a full color table editor and is provided so the user can create/modify custom color enhancement tables. The user has the ability to change a single color or a range of colors by directly changing the intensities of the three color guns. Color tables can be saved and/or retrieved to/from a file.

Animation provides a menu of selections for looping PPI and/or CAPPI displays. A slider bar can be used to control the speed of the animation. Animation

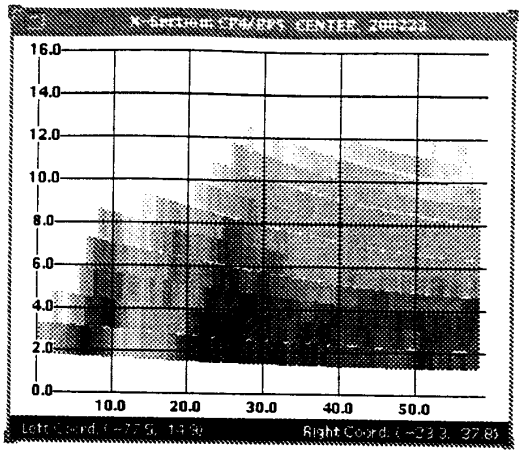

Fig 5: Sample vertical cross section display.

frames can be saved to file for later display.

Clear is used to restore the PPI/CAPPI window to the state prior to any overlaying.

4. SUMMARY

The Interactive Radar Analysis Software (IRAS) package has been successfully ported to the Sun SPARCstation. Its performance and capabilities are far superior to those found on its PC predecessor. The user interface is much easier to use and customize for specific applications. Sun-IRAS is available, at no cost, to anyone with Internet access via anonymous ftp. Anyone interested in getting a copy or receiving information on updates can address e-mail to *dave@nimbus.ias.sdsmt.edu*..

Acknowledgments. The development effort has been supported by NOAA-North Dakota Cooperative Agreement NA17RA0218-01 and contract ARB-IAS-91-2 with the North Dakota Atmospheric Resource Board, under the Federal-State Cooperative Program in Atmospheric Modification Research and by the National Science Foundation under grants ATM-8720252 and ATM-9022846.

REFERENCES

Corbet, J., and C. Mueller, 1991: *zeb*: software for data integration, display, and analyses. Preprints, 25th Int'l Radar Meteor. Conf., Boston, Amer. Meteor. Soc., 216-219.

Oye, R., and R. Carbone, 1981: Interactive Doppler editing software. Preprints, 20th Conf. on Radar Meteor., Boston, Amer. Meteor. Soc., 683-689.

Priegnitz, D., 1991: The Interactive Radar Analysis Software (IRAS) package. Preprints, Seventh Int'l Conf. on Interactive Information and Processing Sys. for Meteor., Oceano., and Hydrol., Boston, Amer. Meteor. Soc., 173-176.

Reprinted from the preprint volume of the 26th International Conference on Radar Meteorology, 24-28 May 1993, Norman, OK. Published by the American Meteorological Society, Boston, MA.

13.2

APPENDIX K

AN UPDATE ON WEATHER RADAR SYSTEM SENSITIVITY

Paul L. Smith

Institute of Atmospheric Sciences
South Dakota School of Mines and Technology
501 E. St. Joseph Street
Rapid City, South Dakota 57701-3995

1. INTRODUCTION

The myth that "short-wavelength radars are more sensitive than long-wavelength radars" seems firmly entrenched in the lore of radar meteorology. It evidently stems primarily from the expression for the Rayleigh-scattering cross section of a spherical drop of diameter D:

$$\sigma = \pi^5 |K|^2 D^6 / \lambda^4 \qquad (1)$$

Thus, statements such as "... the return from rain is proportional to the fourth power of the frequency" (Michelson *et al.,* 1990) continue to appear in the literature.

Neither side-by-side comparisons (e.g., Hobbs *et al.,* 1985) nor tabulations of system performance characteristics support this view of weather radar sensitivity. In Table 12-1a of Gossard and Strauch (1983) the most sensitive radar of the nine listed (with wavelengths from 0.86 to 23 cm) operated at the longest wavelength. Moreover, its margin of sensitivity over the 0.86 cm radars tabulated was more than 20 dB, whereas (1) alone would favor the shorter-wavelength systems by 57 dB. One might well wonder what happened to the "missing" 77 dB?

The answer is that other factors also have significant impact on the overall sensitivity of weather radars. Such factors as the available transmitter power output and receiver sensitivity vary with the wavelength used, and from system to system. Antenna beamwidth constraints may also affect the overall system sensitivity. These issues were examined in Smith (1986), where it was shown that for systems with a specified beamwidth, the apparent advantage of operating at shorter wavelengths indicated by (1) can be more than offset by the other considerations.

Now a new generation of weather radars is in service, operating at wavelengths from 1.3 mm to 6 m. These systems employ modern technology, and some have clearly demonstrated sensitivity better than that of the radars available a decade or more ago. It seems appropriate to examine the sensitivities of these new systems to see whether the same general features still hold.

2. PROCEDURE

It is difficult to establish a consistent basis for sensitivity comparisons involving systems with a wide range of designs and purposes. One convenient way to do this is to calculate the reflectivity factor required to give a specific single-pulse signal-to-noise ratio, taken here to be unity, at a specified range. This clearly ignores the important effects of signal processing on the system sensitivity, about which more will be said later.

The calculations herein use a transposition of (5) from Smith (1986):

$$Z_e = \frac{1024\, k(\ell n\, 2) r^2}{\pi^3 c\, L_r} \left[\frac{\lambda^2}{P_t \tau^2 G^2 \Theta^2} \right] \left[\frac{\alpha\, T_s}{|K|^2 L_a L_m} \right] \frac{\bar{P}_r}{N} \qquad (2)$$

Here the symbols have the usual meanings, with:

- k = Boltzmann constant
- L_a = atmospheric propagation loss
- L_m = microwave loss within system
- L_r = receiver loss due to band pass
- N = equivalent noise power input to receiver
- T_S = system noise temperature
- α = (in effect) ratio of noise bandwidth to $1/\tau$.

The loss factors are numerical values, each ≤ 1. A fixed range of 10 km was used in the calculations, and the value of L_r was taken to be 0.7 (corresponding to a nominal receiver loss of 1.5 dB).

A solicitation for information was sent to the proprietors or operators of a variety of operational or research radars. This yielded responses concerning more than 25 systems operating at wavelengths from 1.3 mm to 6 m. Not all provided

information adequate to make the calculation indicated in (2); in some cases it was possible to infer or estimate needed missing values, but in other cases this could not be done comfortably. For systems with variable parameters (e.g., τ) the calculation used the value most favorable to the sensitivity.

Figure 1 summarizes many of the results of the calculations. The first thing evident is that systems able to detect echoes of -20 dBz or weaker at 10 km are now available at wavelengths from 3 mm to 10 cm. The wavelength dependence indicated by (1), or even the weaker dependence on the square of the wavelength explicit in (2), does not show up in these calculations. (This fact is highlighted by the λ^4 line in the figure.) In fact, across the middle part of the spectrum there appears to be very little difference in the available system sensitivities.

3. CAVEATS AND DISCLAIMERS

These calculations are not intended to be reliable indicators of the specific performance of any given system in any given situation.

- They take no account of the effects of signal processing on sensitivity. Signal integration enhances the system sensitivity, and Doppler processing tends to provide even greater enhancement. Improved signal processing accounts for much of the WSR-88D's operating sensitivity advantage over the WSR-57. In scanning radars, signal processing may favor shorter-wavelength systems because of the shorter time-to-independence involved. However, vertically-pointing wind profilers achieve signal-processing gains of the order of 50 dB with their ability to use quasi-coherent integration and very long dwell times.
- They do not take adequate account of the microwave system losses represented by L_m in (2). For some systems, these losses are subsumed into the measured values of transmitted power, antenna gain, and so forth. In other cases, approximate values were provided, while in still others, no information was furnished and no losses were included. These losses tend to be greater at shorter wavelengths and can have significant effect on system sensitivity, but this depends very much on the overall system configuration. That makes either general statements or useful approximations

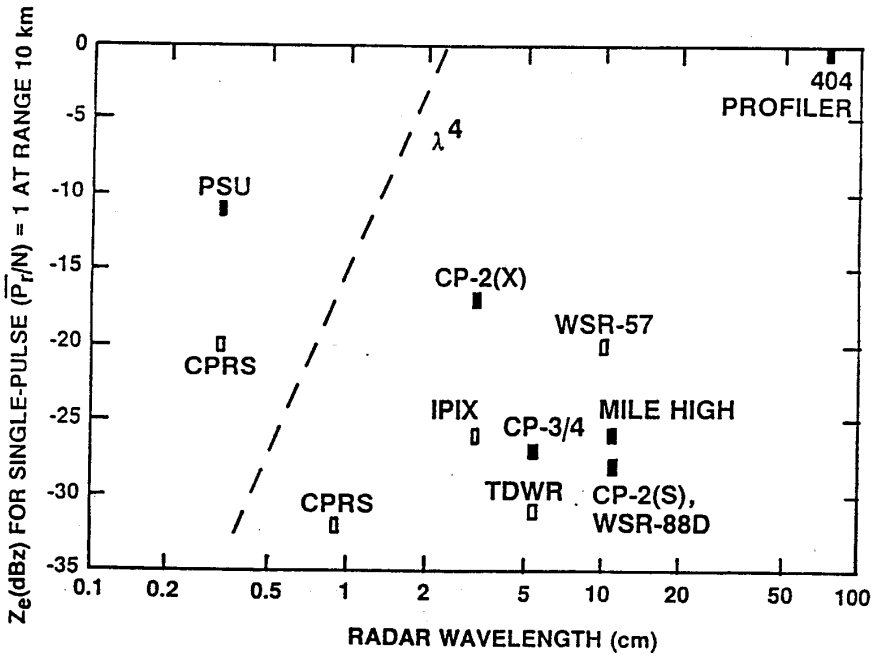

Fig. 1: Plot showing the approximate Z_e required to produce a single-pulse mean signal-to-noise ratio of unity at range 10 km, for a variety of radar systems operating at different wavelengths. Closed symbols indicate systems for which the information supplied was sufficient for a complete calculation; open symbols indicate systems for which some of the needed values were inferred or estimated. Key to less familiar radars: CPRS (U. Massachusetts); IPIX (McMaster U.); PSU (Penn State U.).

difficult in the absence of measured values of the relevant system characteristics.

- They need to be adjusted for atmospheric propagation losses at other ranges, which are noticeable at 10 cm and become serious at wavelengths less than 1 cm. (Since this analysis concerns sensitivity to weak echoes, the issue of attenuation by precipitation is not directly relevant.)

4. DISCUSSION

First of all, these calculations are not intended to be party to any "my radar is more sensitive than your radar" arguments. They are primarily intended to help refute the widespread myth concerning the effect of wavelength on sensitivity. The comparison in Fig. 1 of the sensitivities of radar systems operating over the range of wavelengths from 3 mm to 74 cm demonstrates once again that the Rayleigh scattering law alone is far from sufficient to account for the wavelength variations.

Indeed, over the center part of the range (say 9 mm to 10 cm) systems with essentially the same sensitivity are available at a variety of wavelengths. This behavior was suggested in Smith (1986) for systems with similar antenna beamwidths, as is the case for many of those considered here. Other considerations (e.g., cost, transportability) may be important in selecting an operating wavelength for some particular radar application, and sensitivity alone should not be a dominant factor in choosing the appropriate wavelength.

Acknowledgments. This research was sponsored by the National Science Foundation under Grant No. ATM-9022846 and the NOAA/North Dakota Federal State Cooperative Program under Agreement No. NA 27RA0178-01 through the North Dakota Atmospheric Resource Board. The gracious response from all those who supplied information about their radars is greatly appreciated.

APPENDIX

Presentation of Radar Specifications

One result from the solicitation of information about the various radars was the observation that there is little uniformity in the available descriptions. This adds to the difficulty of trying to make comparisons among systems. Some comments about the information received follow:

- Transmitter characteristics (λ, P_t, τ): Little problem here, except for a tendency to take inadequate account of system losses in connection with P_t.
- Antenna characteristics (G, Θ): Occasionally the values quoted appeared to be a bit optimistic for the size of the antenna used.
- Receiver characteristics (T_s, plus the bandwidth B and/or noise figure F_n and/or MDS as an estimate of M): This was the source of the greatest difficulties. The noise power can be calculated either from $k\ T_s\ B$ or from $k\ T_0\ B\ F_n$ with T_0 = 290 K. Often some of these quantities are not well known, and sometimes not enough information was available to make a calculation. If only T_s or F_n was given, it was assumed that $B \approx 1/\tau$ (i.e., $\alpha \approx 1$). For some systems, a value of B much greater than $1/\tau$ was quoted; those were penalized in the calculation by using an appropriately larger value of α, but that may not be fair in every case. Sometimes values of all four receiver quantities were given, but they were not always consistent (e.g., $T_0\ F_n \neq T_s$; or $k\ T_s\ B \neq$ MDS); in those cases, the combination most favorable to the system sensitivity calculation was employed (with some trepidation).

REFERENCES

Gossard, E. E., and R. G. Strauch, 1983: *Radar Observations of Clear Air and Clouds.* Elsevier Science Publishers, Amsterdam. 280 pp.

Hobbs, P. V., N. T. Funk, R. R. Weiss, Sr., J. D. Locatelli and K. R. Biswas, 1985: Evaluation of 35 GHz radar for cloud physics research. *J. Atmos. Oceanic Tech.*, **2**, 35-48.

Michelson, M., W. W. Shrader and J. G. Wieler, 1990: Terminal Doppler Weather Radar. *Microwave J.*, Feb. 1990, 139-148.

Smith, P. L., 1986: On the sensitivity of weather radars. *J. Atmos. Oceanic Tech.*, **3**, 704-713.

APPENDIX L

CLOUD RADAR SYSTEM SENSITIVITY VERSUS OPERATING WAVELENGTH

Paul L. Smith

Institute of Atmospheric Sciences, South Dakota School of Mines and Technology
501 E. St. Joseph Street, Rapid City, South Dakota 57701-3995

1. INTRODUCTION

The concept for a spaceborne cloud radar system for GEWEX/TRMM II indicates 94 GHz to be the frequency of choice. This choice is indicated to be based on considerations of high sensitivity and high resolution. While the latter is certainly a factor favoring the use of millimeter wavelengths, the sensitivity issue is not so clear-cut.

The myth that "short-wavelength radars are more sensitive than long-wavelength radars" seems firmly entrenched in the lore of radar meteorology. It evidently stems primarily from the expression for the Rayleigh-scattering cross section of a spherical drop of diameter D:

$$\sigma = \pi^5 |K|^2 D^6 / \lambda^4 \quad . \qquad (1)$$

However, neither side-by-side comparisons (e.g., Hobbs *et al.*, 1985) nor tabulations of system performance characteristics (e.g., Gossard and Strauch, 1983) support this view of weather radar sensitivity. Factors other than the operating wavelength also have significant impact on the overall sensitivity of weather radars. The available transmitter power output and receiver sensitivity vary with the wavelength used. Antenna beamwidth constraints may also affect the overall system sensitivity. These issues were examined in Smith (1986), where it was shown that for systems with a specified beamwidth, the apparent advantage of operating at shorter wavelengths indicated by (1) can be more than offset by the other considerations.

2. ANALYSIS

One convenient way to establish a consistent basis for sensitivity comparisons is to calculate the reflectivity factor required to give a specific single-pulse signal-to-noise ratio, taken here to be unity, at a specified range. (This clearly ignores the important effects of signal processing on the system sensitivity.) Such calculations can use a transposition of (5) from Smith (1986):

$$Z_e = \frac{1024\, k(\ell n\, 2) r^2}{\pi^3 c\, L_r} \left[\frac{\lambda^2}{P_t \tau^2 G^2 \Theta^2} \right] \left[\frac{\alpha\, T_s}{|K|^2 L_a L_m} \right] \frac{\overline{P}_r}{N} \qquad (2)$$

Here the symbols have the usual meanings, with:

- k = Boltzmann constant
- L_a = atmospheric propagation loss
- L_m = microwave loss within system
- L_r = receiver loss due to band pass
- N = equivalent noise power input to receiver
- T_S = system noise temperature
- α = (in effect) ratio of noise bandwidth to $1/\tau$.

The loss factors are numerical values, each ≤ 1. A fixed range of 10 km was used in the calculations herein, and the value of L_r was taken to be 0.7 (corresponding to a nominal receiver loss of 1.5 dB).

Calculations have been made for more than 25 operational or research radar systems operating at wavelengths from 1.3 mm to 6 m. Figure 1 summarizes many of the results of the calculations. The first thing evident is that the wavelength dependence indicated by (1), or even the weaker dependence on the square of the wavelength explicit in (2), does not show up in these results. (This fact is highlighted by the λ^4 line in the figure.) Across the middle part of the spectrum there appears to be very little difference in the available system sensitivities. More importantly for present purposes, systems operating at wavelengths of 0.86 cm or greater offer sensitivity advantages of more than 10 dB over the currently-available 3-mm systems.

These calculations take no account of the effects of signal processing, which generally tends to enhance system sensitivity. Signal processing effects can favor shorter-wavelength systems because of the shorter time-to-independence involved, but orbital motion of a spaceborne radar negates this factor. The calculations also do not take adequate account of the microwave system losses represented by L_m in (2). These losses tend to be greater at shorter wavelengths and can have significant effect on system sensitivity, but this

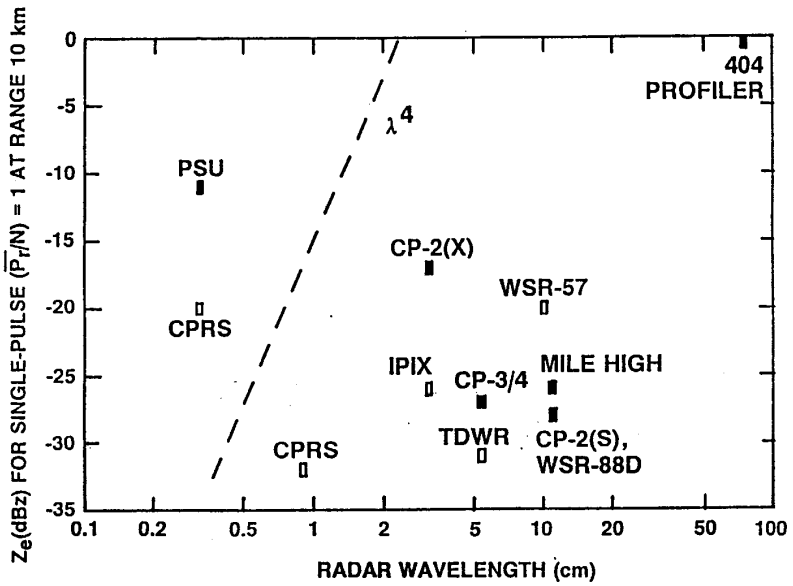

Fig. 1: Plot showing the approximate Z_e required to produce a single-pulse mean signal-to-noise ratio of unity at range 10 km, for a variety of radar systems operating at different wavelengths. Closed symbols indicate systems for which the information supplied was sufficient for a complete calculation; open symbols indicate systems for which some of the needed values were inferred or estimated. Key to less familiar radars: CPRS (U. Massachusetts); IPIX (McMaster U.); PSU (Penn State U.).

depends very much on the overall system configuration. The atmospheric propagation losses represented by L_a become increasingly serious at wavelengths less than 1 cm.

3. DISCUSSION

The comparison in Fig. 1 of the sensitivities of radar systems operating over a wide range of wavelengths demonstrates once again that the Rayleigh scattering law alone is far from sufficient to account for the wavelength variations. Other considerations (e.g., cost, transportability) may be important in selecting an operating wavelength for a particular radar application, and sensitivity should not be a dominant factor in choosing the appropriate wavelength.

On a spacecraft, antenna size is likely to be a major limiting factor. Suppose that a given antenna aperture is available for either a 3.2-mm or an 8.6-mm system; the beamwidth for the latter would be a factor 2.7 greater. If the targets of interest are no wider than the footprint of the 3.2-mm beam, then according to (2), the relative sensitivity of the 8.6-mm system would be degraded by about 8-9 dB. That would make the two systems roughly comparable in sensitivity, according to Fig. 1. Along-path attenuation, however, would have a much greater effect on the 3.2-mm system.

The implication of this analysis is that the question of overall system performance should be carefully examined before the operating frequency for the contemplated cloud radar is selected.

Acknowledgments. This research was sponsored by the National Science Foundation under Grant No. ATM-9022846 and the NOAA/North Dakota Federal State Cooperative Program under Agreement No. NA 27RA0178-01 through the ND Atmospheric Resource Board.

REFERENCES

Gossard, E. E., and R. G. Strauch, 1983: *Radar Observations of Clear Air and Clouds.* Elsevier Science Publishers, Amsterdam. 280 pp.

Hobbs, P. V., N. T. Funk, R. R. Weiss, Sr., J. D. Locatelli and K. R. Biswas, 1985: Evaluation of 35 GHz radar for cloud physics research. *J. Atmos. Oceanic Tech.*, **2**, 35-48.

Smith, P. L., 1986: On the sensitivity of weather radars. *J. Atmos. Oceanic Tech.*, **3**, 704-713.

APPENDIX M

THE USE OF A TWO-DIMENSIONAL, TIME-DEPENDENT CLOUD MODEL TO PREDICT CONVECTIVE AND STRATIFORM CLOUDS AND PRECIPITATION

Fred J. Kopp and Harold D. Orville

Institute of Atmospheric Sciences
South Dakota School of Mines and Technology
501 E. St. Joseph Street
Rapid City, SD 57701-3995

ABSTRACT

A two-dimensional, time-dependent cloud model has been used in two field projects to forecast the convective development during the day from the morning sounding. In effect, the cloud model gives a dynamic analysis of the sounding as affected by heating and evaporation at the earth's surface, divergence of the winds throughout the atmosphere, and cloud shadow effects. During the initial project, the Cooperative Huntsville Meteorological Experiment, the results were mixed. Model runs were easily made when soundings were available, but displaying the results in a meaningful and useful way was the limiting factor. In a later experiment, the North Dakota Thunderstorm Project, the problem of displaying results was overcome and soundings were available from the local weather service forecast office with a high degree of reliability. The experimental model correctly forecasts convective development about 80% of the time, and precipitation or no precipitation more than 70% of the time.

APPENDIX N

THE USE OF CLOUD MODELS FOR THE PREDICTION OF LOCAL CLOUD AND PRECIPITATION CONDITIONS

Harold D. Orville, Fred J. Kopp, Richard D. Farley
and Gerald M. Kraaijenbrink

Institute of Atmospheric Sciences
South Dakota School of Mines and Technology
Rapid City, South Dakota 57701-3995

1. INTRODUCTION

The development of cloud models and faster computers is reaching a point where real-time simulation can be made for forecasting purposes. Three-dimensional models are, as yet, too large for routine runs of this nature, but two-dimensional models can be run with a modest requirement for computing resources. Brooks *et al.* (1992) addresses some of the issues involved in the use of this capability, in particular, its limits. On the cloud scale, predicting the location, timing, and intensity of a storm requires an initialization capability that is beyond present data bases that are gathered on a routine basis. However, cloud models can produce generic forecasts of cloud development with modest data input requirements.

That two-dimensional cloud models can produce a generic simulation of cloud growth has been well established by Orville (1965), Orville (1968), Orville and Sloan (1970), Kubesh *et al.*, (1988), and Farley *et al.* (1989).

This paper will report on the results of using a two-dimensional cloud model in a generic forecasting mode; that is, the model is initialized with a sounding and it then forecasts the cloud development that may develop in the vicinity of the sounding. Note that no claim is made that the cloud will form at the location where the sounding was made; rather, the cloud may be observed somewhere nearby, within about 100 km distant. Comparisons will be made with the Bismarck National Weather Service Office observations and the computer model runs made during the North Dakota Thunderstorm Project.

2. MODEL DESCRIPTION

The theoretical framework is a deep-convection, two-dimensional, time-dependent cloud model which has been applied to a variety of atmospheric situations. A density weighted stream function has been used to extend the model to deep convection. Atmospheric wind, potential temperature, water vapor, cloud liquid, cloud ice, rain, snow, and graupel/hail (in the form of ice pellets, frozen rain, graupel, and small hail) are the main dependent variables. The nonlinear partial differential equations constituting the model include the horizontal and vertical equations of motion, a thermodynamic equation, and water conservation equations (for its three phases). The model has been developed from the work of Orville (1965), Liu and Orville (1969), Wisner *et al.* (1972), Orville and Kopp (1977), and Lin *et al.* (1983).

The bulk-water microphysical scheme employed in the model is based on concepts suggested by Kessler (1969) and divides water and ice hydrometeors into five classes: cloud water, cloud ice, rain, snow, and high density precipitating ice (graupel/hail). These five classes of hydrometeors interact with each other and water vapor through a variety of crude parameterizations of the physical processes of condensation/evaporation, collision/coalescence and collision/aggregation, accretion, freezing, melting, and deposition/sublimation. Rain, snow, and graupel/hail, which are assumed to follow inverse exponential size distributions, possess appreciable terminal fall velocities. Cloud water and cloud ice have zero terminal velocities and thus travel with the air parcels. For a detailed discussion of the microphysical processes and parameterizations employed in the bulk water model, the reader is referred to Wisner *et al.* (1972), Orville and Kopp (1977), and Lin *et al.* (1983). The model has been used extensively for the past 10 to 15 years on such topics as cloud modification, hailstorm simulations, microbursts, and excess vapor and heat effects on severe storms.

The model has been designed such that mesoscale convergence can be superimposed in the lower levels and divergence in the upper levels (or vice versa), which can result in stratus-type clouds being formed under certain atmospheric conditions. The manner in which mesoscale convergence is applied to the model and further details of the hydrodynamic equations can be found in Chen and Orville (1980).

Corresponding author address: Harold D. Orville, Institute of Atmospheric Sciences, S.D. School of Mines and Technology, Rapid City, SD 57701-3995.

TABLE 1

Comparison of Model and Observational Data

	NATIONAL WEATHER SERVICE, BISMARCK, ND				MODEL SIMULATIONS			
Date	Cloud Type	Rain	Cloud Base Height (km)	Upper Cloud Height (km)	Cloud	Rain	Cloud Base Height (km)	Cloud Top Height (km)
12-Jun	Cu,Sc,Ac,TCu	Rw-	.5-.9	2.1	TCu	Rw-	0.6	6.0
13-Jun	St,Sc-ovc	L-,R-	.1-.5,.9	1.0	St,Sc-ovc	Rw-	0.4	8.5
14-Jun	Cu, Ci		1.5-2.0	7.6	Cu		1.2	3.8
15-Jun	Ac,Accas,Ci,Cs	Virga	2.4	7.6	down			
16-Jun	Cu,Ac,Accas,Cs,Ci	Virga,Rw-	.9-2.7	7.6	none			
17-Jun	Cu,Ac,Sc,Cs,Cufra	Rw-	.5-1.2	2.4-7.6	Cb	Rw-	1.0	10.0
18-Jun	Ac,Sc,Cu,Ci	Virga,Rw-	1.5-2.4	3.7-7.6	Cu,TCu	Rw-	2.2	3.5
19-Jun	Ac, Accas,Ci,Cs		2.4	7.6	Ac		2.6	3.0
20-Jun	Ac,Sc,Accas,Sc,Ci,Cs	Virga	.9-3.0	7.6	none			
21-Jun	Sc,Cu,Ac,Cs	Rw-,R-	.6-2.0	2.7	Cb	Rw-	2.5	12.0
22-Jun	Cu,Cb,Ac,Ci	Rw-	1.4-1.8	3.0-7.6	Cu,Cu+	Rw–	1.3	4.5
23-Jun	Cu,Cb,Ac,Ci,Cs	Rw-	.9-2.1	7.6	TCu	Rw-	1.5	6.5
24-Jun	Cs,Ac,Cb,TCu,Sc	Rw-	1.2-2.4	3.0	Ac,Cb	Rw-	3.0	8.5
25-Jun	Sc,TCu,Cu,Cb,Ac,Ci	Rw-	.9-1.8	3.7-7.6	TCu	Rw-	1.0	8.0
26-Jun	Sc,Cu,Ac,Cs		.9-2.7	7.6	down			
27-Jun	Ac,Cu,TCu,Cb,Ci	Rw-	1.5-1.8	3.0-7.6	Cu	Virga	2.2	4.0
28-Jun	Accas,Cb,Ci	Rw-,A	1.2-3.0	7.6	Cb	Rw-	2.0	13.0
29-Jun	Ac,Cs,Cu,Ci		1.5-2.0	3.0-7.6	Cu		2.0	5.0
30-Jun	Ci,Cu		1.5-2.0	7.6	TCu	Rw-	2.0	7.0
1-Jul	Cu,Cb,Ci,Sc,Ac,Tcu	Rw-	1.5-2.4	3.0-7.6	Cu,Tcu,Cb	Rw-	2.0	10.0
2-Jul	Accas,Tcu,Ci,Cb	Rw-	2.0	3.0-7.6	Cu,Tcu,Cb	Rw-	2.0	10.0
3-Jul	Accas,Ac,Ci		3.0-3.7	7.6	down			
4-Jul	Ac, Cu,Tcu	Virga	2.7-3.0	7.6	Cu,Tcu	Rw-	2.4	9.0
5-Jul	Ac, TCu,Cu,Cb,Cs	Rw-	1.8-2.7	7.6	Cu,Cb	Rw-	3.0	13.0
6-Jul	Sc,Cb,Accas,Cu,Cs	Rw-	.6-2.1	3.0-7.6	Sc		1.8	3.0
7-Jul	Ac,Cb,Sc,Accas,TCu	Rw-	.9-2.4	7.6	Cu,Tcu	Rw-	2.2	7.0
8-Jul	Ac,Cs,Tcu		2.4	3.0-7.6	Cu,Tcu,Cb	Rw-	2.2	12.0
9-Jul	Ac,Cs	Virga	3.0	7.6	Cu?		1.8	3.0
10-Jul	Ac,Cs,Sc	Rw-	1.8	3.0-7.6	Cu		1.8	2.4
11-Jul	Cb,Cu,Ac,Cs	Rw-	.6-1.8	7.6	Cu,		1.2	5.0
12-Jul	Tcu,Cu,Ac,Ci	Rw-	1.2-1.5	7.6	Cu,Tcu	Rw-	1.2	6.0
13-Jul	Cu,Accas,Sc,Cs	Rw-	1.8-2.4	7.6	Cu		1.6	3.5
14-Jul	Ac,Cu,Sc,Cs	Rw-	1.5 - 1.8	3.0-7.6	Cu,Tcu	Rw-	1.6	8.0
15-Jul	Cu,Ci		1.7 - 1.8	7.6	Cu		1.8	5.0
16-Jul	Cu,Ac,Sc,Ci		1.5 - 1.8	7.6	Cu		2.1	4.0
17-Jul	Sc,Cu,Ac,Cs	Rw-	.3 - 1.2	7.6	Cu,Tcu,Cb?	Rw-	1.5	8.0
18-Jul	Sc,Cu,Tcu,Ac		.3 - 1.8	7.6	Cu,Tcu	Rw-	1.0	6.0
19-Jul	Ac,Cu		1.8	2.7	Cu.,Tcu ,	Rw-	1.8	7.0
20-Jul	Cu,Cs,Ci		1.5	7.6	Cu		2.1	3.0
21-Jul	Ci			7.6	Cu		2.2	3.4
22-Jul	Cs,Ci			7.6	Cu		2.2	3.0

Atmospheric sounding conditions of temperature, humidity, and wind are needed to initialize the model. Surface heating and evaporation rates may also be specified (as described in Liu and Orville, 1969). If information is available on larger scale convergence/divergence patterns, then these data can also be used in model runs.

2.1 Heating at the Surface

The model uses a heat flux technique at the surface to warm the lower atmosphere and to eventually lead to convection. This method has been described recently by Kopp *et al.* (1990).

The surface energy equation (Orville, 1965) has been modified to change the treatment of surface temperature. In our past models, surface temperature was prescribed as a time-changing variable. In these simulations, a constant flux of heat into the surface layer of the model was used and, as the surface layer warms up, was balanced by an eddy transport of heat out of the surface layer.

The energy flux used is about 300 J m^{-2} s^{-1} at the surface. This is a fraction of the short-wave solar energy reaching the surface in the summertime. Sellers (1965) indicates that this is about the average sensible heating that would occur over a relatively dry surface in the summertime.

In the event that clouds are predicted to form, the heating rate is reduced to one-half of the original heating rate at the grid points directly under the clouds. This is a very highly parameterized simulation of the radiative flux of the surface. No attempt has been made to simulate long-wave radiation interactions at the surface, nor has any attempt been made to simulate the time-dependent short-wave variation that occurs as the sun rises, reaches its zenith, and sets.

3. RESULTS

Table 1 contains the National Weather Service data hourly surface weather observations taken at the Bismarck weather office (very close to the project operations center). In Table 1 under the Weather Service observational data, upper cloud refers to the observed height of the cloud layer at the upper levels. In the model results, the cloud top heights are given. These two numbers are not generally comparable except when thunderstorms are creating the upper layer cirrus, perhaps. However, the observations show no clouds above 7.6 km, which seems too low for some cirrus anvils. Clouds were observed every day of the project, although when restricted to the cumulus type of clouds, the number of observations is 36 days. The cloud model predicted 32 days with convective clouds, with 31 of those days being a correct prediction. Model cloud bases were generally within a few hundred meters of the observations, except in three cases. With respect to prediction of cloud development, the model was accurate 85% of the time. Precipitation prediction was less accurate. Precipitation was observed on 26 days during the project. The model predicted precipitation on 23 days with 17 days being correct. Overall, the predictions were correct 71% of the time that there would or would not be precipitation. On days with rain, the model predicted correctly 74% of the time; and on days with no precipitation, the model was correct 67% of the time.

A contingency table using the precipitation results from Table 1 is found in Table 2. The χ^2 value is 6.1. Thus there is a 98% chance that the model forecast is real and not purely random.

TABLE 2

Rain Results

	Observed		
Forecast	Rain	No Rain	Total
Rain	17	5	22
No rain	6	10	16
Total	23	15	38

The timing of the cloud formation and precipitation was not considered. The heating function used in the model represented an average heat flux for the day; it did not vary from zero at sun-up to a maximum in the middle of the day and then back to zero at sunset. Consequently, the heating is too large early in the day and not strong enough during the final stages of the eight hours of simulation. A more realistic heating function should lead to the prediction of the timing of events, but other external factors, such as advection of moisture into the domain, might overwhelm any purely local effect. These are factors for further research and development.

4. CONCLUSIONS

The model both underpredicted and over-predicted convection. Table 2 suggests that there is no predominant tendency with five errors of over forecasting rain and six errors of under forecasting. Examples of over-prediction are June 30, July 4, 8, 18, 19, 21, and 22, while June 16, 20, 27, and July 6, 10, 11, and 13 are underpredictions. The model does not appear to make a systematic error, so the

most probable problem is change in the environmental conditions during the day which is not obvious in the early morning. Changes in the stability or moisture content of the atmosphere during the day will make the model run non-representative of the convection later in the day. Kopp *et al.* (1990) shows that there is a significant variation from day to day in the precipitable water during this project.

Acknowledgments. This work has been supported by the National Science Foundation under Grant No. ATM-8901355 and the National Aeronautics and Space Administration under Grant No. NAG-8-632. NOAA funding is also acknowledged under Contract Nos. ARB-IAS-89-2 and ARB-IAS-92-1 with the North Dakota Atmospheric Resource Board. Thanks are given to the National Center for Atmospheric Research, which is sponsored by the National Science Foundation, for the use of their computers. We also extend our thanks to Joie Robinson for her work in preparing this manuscript.

REFERENCES

Brooks, H. E., C. A. Doswell III, and R. A. Maddox, 1992: On the use of mesoscale and cloud-scale models in operational forecasting. *Weather and Forecasting,* **7**, 120-132.

Chen, C-H., and H. D. Orville, 1980: Effects of mesoscale convergence on cloud convection. *J. Appl. Meteor.,* **19**, 256-274.

Farley, R. D., P. E. Price, H. D. Orville and J. H. Hirsch, 1989: A note on the numerical simulation of graupel/hail initiation via the riming of snow in bulk water cloud microphysical models. *J. Appl. Meteor.*, **28**, 1128-1131.

Kessler, E., 1969: On the distribution and continuity of water substance in atmospheric circulation. *Meteor. Monogr.*, **10**, 32. 84 pp.

Kopp, F. J., H. D. Orville, J. A. Jung and R. T. McNider, 1990: A parameterization of radiation heating at the surface in a numerical cloud model. *Preprints Conf. Cloud Physics,* San Francisco, CA, Amer. Meteor. Soc., J81-J84.

Kubesh, R. J., D. J. Musil, R. D. Farley and H. D. Orville, 1988: The 1 August 1981 CCOPE storm: Observations and modeling results. *J. Appl. Meteor.,* **27**, 216-243.

Lin, Y-L., R. D. Farley and H. D. Orville, 1983: Bulk parameterization of the snow field in a cloud model. *J. Climate Appl. Meteor.,* **22**, 1065-1092.

Liu, J. Y., and H. D. Orville, 1969: Numerical modeling of precipitation and cloud shadow effects on mountain-induced cumuli. *J. Atmos. Sci.,* **26**, 1283-1298.

Orville, H. D., 1965: A numerical study of the initiation of cumulus clouds over mountainous terrain. *J. Atmos. Sci.,* **22**, 684-699.

Orville, H. D., 1968: Ambient wind effects on the initiation and development of cumulus clouds over mountains. *J. Atmos. Sci.,* **25**, 385-403.

Orville, H. D., and F. J. Kopp, 1977: Numerical simulation of the life history of a hailstorm. *J. Atmos. Sci.,* **34**, 1596-1618. [Reply: *J. Atmos. Sci.,* **35**, 1554-1555]

Orville, H. D., and L. J. Sloan, 1970: A numerical simulation of the life history of a rainstorm. *J. Atmos. Sci.,* **27**, 1148-1159.

Sellers, W. D., 1965: *Physical Climatology.* The Univ. of Chicago Press, Chicago, IL. 272 pp.

Wisner, C. E., H. D. Orville and C. G. Myers, 1972: A numerical model of a hail-bearing cloud. *J. Atmos. Sci.,* **29**, 1160-1181.

APPENDIX O

Atmospheric Research, 28 (1992) 271–298
Elsevier Science Publishers B.V., Amsterdam

A status report on weather modification research in the Dakotas

Paul L. Smith[a], Harold D. Orville[a], Bruce A. Boe[b], and Jeffrey L. Stith[c]
[a]*Institute of Atmospheric Sciences, South Dakota School of Mines and Technology, 501 E. St. Joseph Street, Rapid City, SD 57701-3995, USA*
[b]*North Dakota Atmospheric Resource Board, 900 E. Boulevard Avenue, Bismarck, ND 58505-0850, USA*
[c]*Center for Aerospace Sciences, University of North Dakota, Grand Forks, ND 58202-8216, USA*

(Received July 10, 1991; revised and accepted December 15, 1991)

ABSTRACT

Smith, P.L., Orville, H.D., Boe, B.A. and Stith, J.L., 1992. A status report on weather modification research in the Dakotas. In: J.L. Sánchez (Editor), Agriculture and Weather Modification. Atmos. Res., 28: 271–298.

An overview of the status of weather modification research in North and South Dakota (USA) is presented. The operational North Dakota Cloud Modification Project has, since 1976, been seeding summer convective clouds for the dual objectives of hail suppression and rainfall enhancement. Research being carried out as part of a Federal/State cooperative program, in coordination with the operational activities, has included physical and statistical evaluation studies as well as numerical cloud modeling investigations. The statistical analyses provide some indications that the intended seeding effects are being obtained. The physical studies involve aircraft and radar observations and emphasize tracer experiments to study the transport and dispersion of seeding agents and the activation of ice nuclei. The modeling studies simulate the experiments and aid in investigation of the processes involved and the effects of seeding. The 1989 North Dakota Thunderstorm Project, a major field study emphasizing physical and numerical modeling studies, is described briefly.

RÉSUMÉ

Une vue d'ensemble est présentée sur la situation des recherches en modification du temps dans les Dakotas du Sud et du Nord (E.U.A.).

Dans le cadre du plan d'études concernant la modification des nuages dans le Dakota du Nord, des nuages convectifs d'été ont été ensemencés dans le but de supprimer la grêle et d'augmenter la pluie.

Un projet d'études où collaborent des organismes fédéraux et locaux d'Etat, en coordination avec une activité pratique, a contribué à des estimations physiques et statistiques, ainsi qu'à un examen des modèles de nuages. Des analyses statistiques ont fourni certaines indications quant au fait que les effets projetés en ensemençant les nuages se produisent réelement. Les études physiques consistent en observations radar et avion et en expériences à l'aide de traçeurs pour étudier le transport et la disper-

Correspondence to: P.L. Smith, Institute of Atmospheric Sciences, South Dakota School of Mines and Technology, 501 E. St. Joseph Street, Rapid City, SD 57701-3995.

0169-8095/92/$05.00 © 1992 Elsevier Science Publishers B.V. All rights reserved.